UNCLASSIFIED

AD NUMBER

AD844800

NEW LIMITATION CHANGE

TO

Approved for public release, distribution unlimited

FROM

Distribution: USGO: others to Director, Defense Atomic Support Agency, Washington, D. C. 20305.

AUTHORITY

DTRA ltr, 3 Nov 99

THIS PAGE IS UNCLASSIFIED

DASA-2156

RELEVANT LABORATORY EXPERIMENTS

H. Friedman and R. Patrick

RESEARCH REPORT 325
Contract DASA 01-67-C-0131
November 1968

STATEMENT #3 UNCLASSIFIED

Each transmittal of this document outside the agencies of the
U.S. Government must ha...

prepared for

DEFENSE ATOMIC SUPPORT AGENCY
Washington, D. C.

DEC 16 1968

AVCO EVERETT RESEARCH LABORATORY
A DIVISION OF AVCO CORPORATION

40

RELEVANT LABORATORY EXPERIMENTS*

by

H. Friedman and . Patrick

AVCO EVERETT RI .R.H LABORATORY
a div . ion of
AVCO CORPORATION
Everett, Massachusetts

Nove ⁱ ⁱr 1968

prep red for

ABSTRACT

An experiment has been designed to test the basic assumptions of a new model[3] which describes debris motion towards the northern conjugate region from high altitude nuclear explosions. The experimental facility consists of a coaxial plasma source which accelerates ionized aluminum into an environment where the background pressure and magnetic field can be controlled. The initial plasma velocity was 10 cm/μsec, the background magnetic field was varied from zero to 220 gauss and the pressure between 2μ and 50μ in air. These conditions are such that (1) ordinary momentum transfer collisions are unimportant (2) the magnetic pressure is negligible as compared to dynamic plasma pressure and (3) the only momentum exchange mechanism is charge exchange collisions in the presence of a magnetic field. Ultraviolet radiation from the plasma source preionizes the background gas producing an Alfven speed based on the ion density which is less than the plasma velocity. The ambient magnetic field is swept up by aluminum plasma and provides the mechanism for charge exchange momentum exchange process. We find that the aluminum plasma is decelerated with the addition of a magnetic field nearly parallel to the plasma motion. The deceleration rate is proportional to the background pressure. Finally, we note that the charge exchange pickup is effective even at relatively low magnetic fields where the air-ion gyro radius based upon initial plasma velocity is several times the plasma scale length.

TABLE OF CONTENTS

BLANK PAGE

I. INTRODUCTION

In the study of high altitude nuclear explosions, the motion of ionized debris along the earth's magnetic field is not well understood. It is vital to the problem of radar blackout that we be able to predict the debris deposition resulting from such explosions.

Several theories and calculations have been constructed to explain this motion and it is the purpose of this experimental program to simulate some of the effects associated with high altitude nuclear explosions in order that the basic assumptions of these theories may be better understood. To this end, we produce an unsteady, high velocity flow of ionized material along a static magnetic field in an environment where ordinary momentum transport collisions are unimportant. In this situation, transfer of momentum can only occur as a result of charge exchange and ionizing collisions in the presence of a magnetic field.

The focal point of this experiment is the use of electromagnetic forces in the form of a magnetic accelerator to ionize and accelerate a known amount of metallic ion plasma. With this type of plasma accelerator it is possible to impart many thousands of joules to milligram masses, thereby attaining speeds relevant to the study of high altitude nuclear explosions. This capability is not presently available with other energy sources such as converging laser beams.

To perform a relevant laboratory experiment, the following criteria are necessary:

1. The velocity of the ionized material must be of the order of 10^7 cm/sec or higher. At this velocity, the charge exchange and direct ionization cross sections are much greater than those of ordinary gas dynamic collisions.

2. The background gas pressure must lie in the range $1\mu < p < 45\mu$. The upper bound insures that the mean free path for gas dynamic collisions is much larger than the flow scale (30 cm). The lower bound is added to provide sufficient interaction with the background gas within the scale of the experiment (~ 3 meters).

3. The ion gyro radius must be smaller than or equal to the flow scale so that the magnetic field can play an effective role in the momentum transfer process.

4. The magnetic energy of the static field must be much less than the kinetic energy of the plasma so that the magnetic field does not directly

influence the plasma motion. The magnetic field is solely an intermediary agent in the momentum transfer process as is the case in high altitude nuclear debris motion.

5. The energy associated with the convected B field imbedded in metal plasma must also be smaller than the kinetic energy of the debris. We wish to study the motion of ionized debris without the added complication of a "magnetic piston" behind it. The electric currents in the plasma necessary to sustain the jump in magnetic field would unduly complicate the experiment.

6. It is desirable to have a preionization of the ambient air available before the metal ion plasma interacts with it. This will establish a relatively low Alfven speed ahead of the debris, based on the ion density and B field ahead of the expansion. The velocity of the metal ion plasma is greater than the Alfven speed ahead, similar to the conditions for actual high altitude debris motion. In this experiment, the violent discharge in the accelerator creates sufficient ultra-violet radiation to ionize five percent of the background gas at a distance of 1 meter from the plasma source.

The most significant question to be answered by this experiment is: Can the magnetic field which is aligned parallel to the flow affect the motion of the ionized debris and if so, how, in detail, is this accomplished? The second half of this question involves a knowledge of the magnetic field configuration which accompanies the debris motion. Once this magnetic field interaction is established, it then remains to determine the functional behavior upon the parameters of background gas pressure and ambient magnetic field.

II. DESIGN OF EXPERIMENT

The power requirements for the plasma accelerator are essentially fixed by the plasma velocity and the requirement that the ion gyro radius be smaller than or comparable to the flow scale in the following manner. The power unit area of the expanding debris bubble is given by the dynamic pressure of the ambient gas multiplied by the expansion velocity. Thus, the total power expended by the expanding bubble is approximately

$$P \cong (\rho v^2)\,(v)\,(4\pi R^2) \tag{1}$$

where ρ = background density
v = expansion velocity
R = bubble radius

The background density is fixed by restriction on the ion gyro radius, i.e., that

$$\frac{r_i}{R} \lesssim 1 \tag{2}$$

where r_i is given by

$$r_i = \frac{v}{\omega} = \frac{v}{Bq_i}\,m_i \tag{3}$$

and q_i and m_i are the charge and mass of an ion. Also we must have the dynamic pressure, ρv^2, larger than the ambient magnetic field pressure $B^2/2\mu_o$, i.e.,

$$\beta = \frac{\rho v^2}{\dfrac{B^2}{\mu_o}} \gg 1 \tag{4}$$

Solving for ρ and substituting into Eq. (1), one obtains the power for the accelerator

$$P = \frac{4\pi}{\mu_o}\left(\frac{m_i}{q_i}\right)^2 \left(\frac{R}{r_i}\right)^2 v^3\,\beta \tag{5}$$

-3-

Assuming an average ion mass of 20 and velocity of 10^5 m/sec, it can be seen from Eq. (4) that the minimum (i.e., $R/r_i = 1$) power requirement is $5 \times 10^7 \beta$ watts.

The time scale of the experiment and therefore the energy input, is chosen to give a debris bubble of convenient size. To expand at 10^7 cm/sec to a diameter of 30 cm, 3 μ sec are required. If one chooses $(R/r_i)^2 \beta \approx 30$ then this corresponds to an input energy of 1500 joules.

The design for the plasma source which fulfills these power and energy requirements is shown schematically in Fig. 1. The power delivered to the accelerator is

$$P = VI \tag{6}$$

where V voltage across the accelerator and I is the current through it. The voltage is given by

$$V \cong v \, B_{TOT} \, r \tag{7}$$

where $B_{TOT} = \sqrt{B_z^2 + B_\theta^2}$

$B_\theta = \mu_o I/(2 \pi r)$

r $=$ anode radius

The z component of the magnetic field which is externally applied by a coil surrounding the accelerator, serves two purposes; the axial magnetic field (1) limits the heat transfer to the anode and increases the efficiency of the arc and (2) provides a smooth transition to the ambient magnetic field which is applied within the test section.

Under the normal operating conditions when B_z in the accelerator is comparable to or less than B_θ, a power level of 10^9 watts corresponds to a voltage and current of 10 kV and 100 kA respectively. These input requirements are supplied by a fast (1 μ sec rise time) capacitor bank containing 10,000 joules at 50 kV. It follows that approximately

$$\frac{10 \text{ kV}}{50 \text{ kV}} \times 10,000 \text{ joules} = 2000 \text{ joules}$$

are delivered to the plasma accelerator.

It is desirable to have a reproducible mass of ions to be accelerated. The amount of mass is fixed by the input energy and exhaust velocity requirements, i.e.,

$$m = \frac{2}{v^2} = \frac{2 \cdot 2000 \text{ joules}}{10^{10} \text{ m}^2/\text{sec}^2} = .4 \text{ milligram}$$
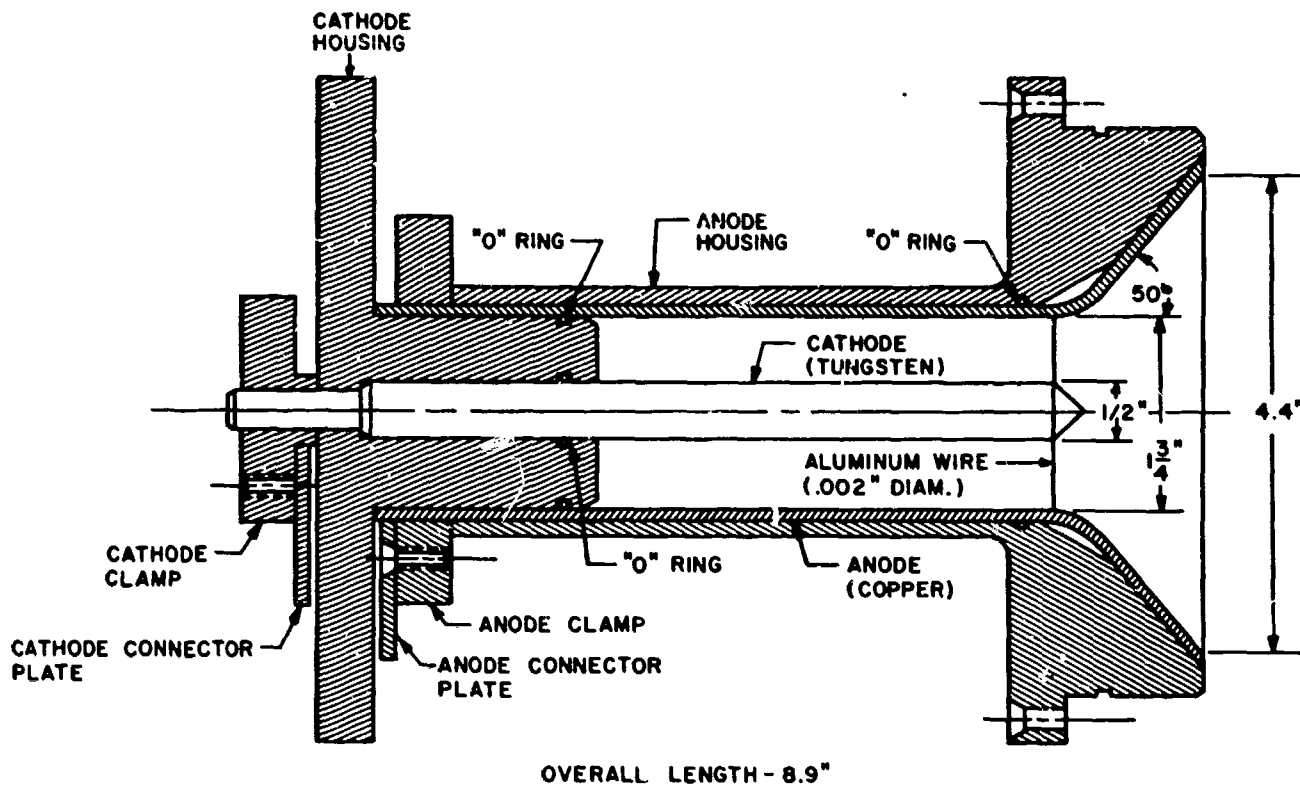
-4-

Fig. 1   Plasma Accelerator

and a simple method of introducing this mass (in the form of thin wires) into the accelerator is shown in Fig. 1. A better method might be the use of foils; however, the low mass requirement forces the use of very thin foils and there is no simple method of placing a foil in the arc. The wires, on the other hand, are simply tied around the cathode and rest upon the anode.

There are two factors which aid in rapidly distributing the ionized material symmetrically around the arc prior to acceleration. Both mechanisms rely upon the observation that since the propelling force on the ionized aluminum is IB_θ and $B_\theta \propto I$, this force is proportional to I^2. Furthermore, since $I \propto \sin \omega t$, at early times,

$$\text{Force} \propto \frac{d^2 x}{dt^2} \propto t^2$$

where x represents the axial position of the ionized mass. Upon performing two quadratures, it follows that $x \propto t^4$ and a simple calculation shows that the ionized mass has traveled only the order of a few cm, by the time the current pulse has passed its maximum and decreased substantially to zero. The ionized mass has not yet left the vicinity of the accelerator when the arc currents vanish. The second half cycle currents restrike on the insulator and the plasma has kinetic energy with essentially no B field energy.

The first symmetrizing factor is the axial bias field. The axial bias field is supplied from a slow (5 millisecond) capacitor bank, and as a result, this field is essentially constant over the entire time scale of the discharge. Now, at the beginning of the arc discharge cycle, when the current and therefore, B_θ, is low, the ionized material is spun in a tight spiral by the axial bias field. By the time the arc current is sufficiently strong to propel the ionized mass out of the arc region, azimuthal symmetry should be achieved.

The second factor aiding symmetry is the instabilities associated with exploding wires. With the passage of 10^5 amps, the wire should definitely be kink unstable in times shorter than 1μ sec. Instabilities of this type should help distribute the plasma around the arc.

Image converter photographs taken at $1/2 \mu$ sec after initiation of the arc current with exposure times of 50 nanoseconds do not show any gross asymmetries in the arc discharge and we conclude that these wires represent a simple, adequate method of reproducibly introducing a known amount of material into the arc.

The pressure of the background gas is determined in such a manner so as to slow the debris in a distance which is convenient with the experimental facility. The debris will slow down appreciably if it picks up a mass of air equal to its initial weight (.4 mg). Assuming a bubble diameter of 30 cm and complete mass pickup, this pickup requirements corresponds to an air pressure of $\sim 10 \mu$.

Figure 2 shows a schematic diagram of the experimental facility including some of the diagnostic devices. The time constant of the slow capacitor bank is long enough to permit the (axial bias) magnetic field to penetrate the copper anode and connect smoothly with the (ambient) magnetic field produced by the field coils. A time delay generator switches on the fast bank when the ambient field has reached its maximum.

The main diagnostic devices are a set of rotating mirror cameras and various magnetic field probes. The cameras have a maximum writing speed of 1 cm/sec can resolve velocities equal to 10 cm/μ sec and the location of the two cameras provide an almost continuous field of view for the first meter of travel. The magnetic field probes are "center tap" grounded and are operated "push-pull" to eliminate electrostatic pickup.

An important monitoring device is a tungsten U. V. detector which is located on the rear wall of the tank opposite the accelerator. This detector gives the level of U. V. radiation resulting from the violent breakdown of the aluminum plasma, in the wavelength range 200-1200 Å. From this information, the initial ionization level of the background gas can be calculated. It is to be noted that high altitude nuclear explosions also produce a high level of background ionization as a result of x-radiation.
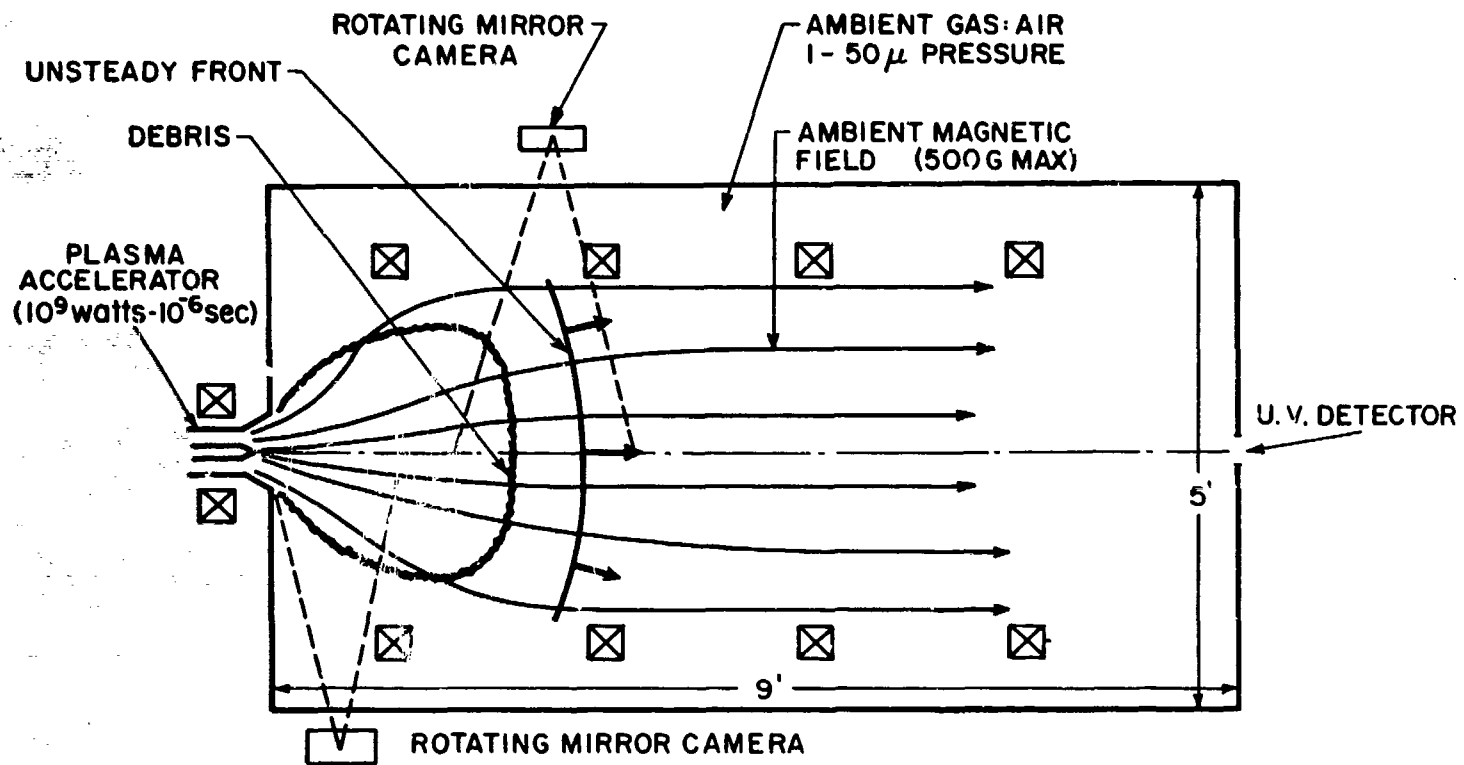
Fig. 2   Schematic Diagram of Experiment at Facility

B2479

III. EXPERIMENTAL RESULTS

1. Accelerator Performance

Voltage and current measurements made at the plasma accelerator indicate its performance is in accordance with design specifications. The peak voltage across the accelerator was measured to be ~ 5 kV. The current signal, on the other hand, exhibits a quarter cycle of $\tau = 1.5 \, \mu$ sec which indicates a peak current of

$$I \cong \frac{c V_o \pi}{2 \tau} \cong 2 \times 10^5 \text{ amps}$$

where V_o = 30 kV is the capacitor voltage. Thus, the average (RMS) power is approximately $1/2 \times 10^9$ watts which gives an input energy of 1,500 joules for the first 1/2 cycle.

Assuming that all this input energy is converted into kinetic energy of the aluminum debris (the validity of this assumption has been confirmed by optical and field probe data and will be discussed shortly), the exhaust velocity of the ionized aluminum is approximately

$$v_{exhaust} \cong \sqrt{\frac{2}{m} \, \mathcal{E}_{input}} \cong 10^5 \text{ m/sec}$$

for $m = 4 \times 10^{-7}$ kg.

The E/B drift velocity in the nozzle region of the anode is consistent with this exhaust velocity. The azimuthal magnetic field in the annulus is approximately

$$B_\theta \cong \frac{\mu_o I}{\pi R} \cong 1.6 \text{ web/m}^2$$

where R = .05 m is the anode radius and the radial electric field is approximately

$$E_r \cong \frac{V}{r} \cong 2 \times 10^5 \text{ volts/m}$$

where $r \cong 2.5$ cm is the annular spacing and V = 5 kV is the accelerator voltage. These two orthogonal fields given an E/B drift velocity in the axial direction of ~ 10^5 m/sec.

A further check of the accelerator performance was made by firing the plasma into a high pressure background with no applied field and observing the resultant motion. For background pressures of the order of 1 mm, the density is sufficiently high so that all of the ambient gas is picked up via standard momentum transfer collisions and a simple theory which conserves momentum should predict the debris motion.

Figure 3 shows the data which is an x-t diagram obtained from a rotating mirror camera along with a pencil sketch of the data.

The philosophy of the calibration measurement is to calculate the initial mass in the accelerator from the high pressure mirror camera data and compare that with the mass of aluminum wire strung across the gap.

The conservation of momentum when applied to the aluminum mass when thermal effects are neglected and one dimensional flow is assumed is given by

$$[m_o + m(z)] \, v(z) = m_o v_o \tag{8}$$

where m and v are the mass and velocity and the subscript zero refers to their initial values. $m(z)$ is the mass of ambient gas picked up by the aluminum and is proportional to the volume swept out. The volume swept out at high pressures is essentially a cone with base radius approximately one third times that of its height. This data was determined using an S.T.L. image converter camera. The picked up mass is

$$m(z) = \rho_{air} \, \pi \, z^2/27 \tag{9}$$

where ρ_{air} is the air density at 1 mm. Substituting Eq. (9) into Eq. (8) and integrating the result once, the initial mass is expressed as

$$m_o = \frac{\pi}{108} \, \rho_{air} \, \frac{z^4}{(v_o t - z)} \tag{10}$$

The initial velocity is estimated from the first 10 cm of travel and the resultant m_o is plotted in Fig. 3. The aluminum mass put into the accelerator is 4×10^{-7} kg. The inferred mass from the mirror camera data is fairly constant and agrees well for the first 20 cm of travel. After that, the plasma has slowed sufficiently so that its kinetic energy has been converted to thermal energy. Beyond this point, a blast wave solution should be used. In the blast wave model plasma pressure exert a force on the combined aluminum and air mass and this decreases the deceleration and appears as an effective increase in m_o in Eq. (10).

With the simple method of introducing a known amount of aluminum and this calibration technique, this accelerator can be used as reliable
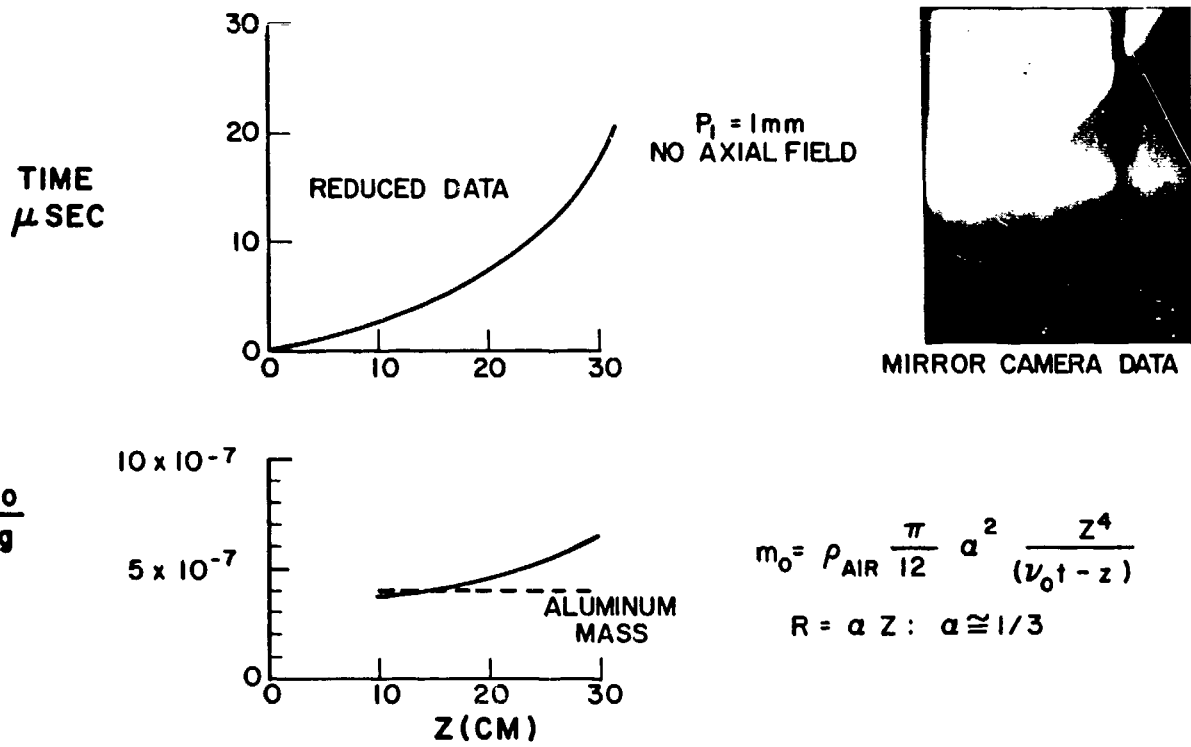
TIME
μ SEC

REDUCED DATA

$P_1 = 1mm$
NO AXIAL FIELD

MIRROR CAMERA DATA

$\frac{m_0}{Kg}$

10×10^{-7}

5×10^{-7}

ALUMINUM MASS

$m_0 = \rho_{AIR} \frac{\pi}{12} \alpha^2 \frac{z^4}{(\nu_0 t - z)}$

$R = \alpha Z : \alpha \cong 1/3$

Z(CM)

Fig. 3   High Pressure Accelerator Calibration

-11-

tool for high velocity plasma research. The attainment of exhaust velocities of 10^5 m/sec as indicated by accelerator voltage and current measurements and confirmed by optical and field probe data (in the next section) show that the accelerator operates at high efficiency and that the performance can be predicted by simple energy and momentum considerations.

2. Initial Conditions

The electrical breakdown of the aluminum wire along with the passage of the order of 10^5 amperes in each wire results in the emission of a pulse of radiation which preionizes a fraction of the ambient gas in much the same manner as x-radiation ionizes the atmosphere in high altitude nuclear explosions. A tungsten ultraviolet detector was mounted at the rear of the tank facing the accelerator and the amount of radiation in the range 200-1200 Å was recorded.

The power incident on the U. V. detector is related to its output current in the following manner:

$$P_{INC} = \frac{I}{e} \frac{\mathcal{E}_\lambda}{\eta_\lambda}$$

where P_{INC} = incident power

$\quad$ I $\quad$ = output current (photo current from tungsten photo cathode)

$\quad$ e $\quad$ = electronic charge

$\quad \eta_\lambda$ $\quad$ = photon efficiency = number of electrons emitted per incident photon

$\quad \mathcal{E}_\lambda$ $\quad$ = photon energy

Assuming an average photon energy (in the range 200-1200 Å) of 15 eV and a photon efficiency of about 10%,[1] the incident power to the detector was found to be ~ 30 watts. The detector area is $A_d = 10^{-1}$ cm and it is located R = ~ 3m from the accelerator. Assuming that the power is radiated in a solid angle of $2\pi R^2$, the peak power radiated by the accelerator in the U. V. range is

$$P \cong (30 \text{ watts}) \frac{2\pi R^2}{A} \cong 2 \times 10^8 \text{ watts}$$

which is approximately 10% of the input power to the accelerator.

To calculate the fractional ionization of the ambient air in the tank we note that for photon energies greater than the ionization potential, the photoionization cross section, σ, is $\sigma \cong 10^{-17}$ cm^2. Thus at pressures of the order of 10μ (density $\cong 3 \times 10^{14}$ cm^{-3}), the photoionization mean free path $\lambda \cong 3$ meters which is larger than the scale of the experiment.

Using a linear approximation, the fractional ionization per second is then given by

$$\% \text{ ionization/sec} = (\text{photon flux}) \, \sigma$$

Since the photon flux varies inversely as the square of the distance from the source, the ionization fraction becomes greater as one approaches the accelerator. The photon flux at the U. V. detector is $\sim 1.2 \times 10^{+19}$ photons/(cm^2 sec) and the photon flux at any point is

$$\text{photon flux} = 1.2 \times 10^{+20} \left(\frac{9}{R^2}\right) \frac{\text{photons}}{\text{cm}^2 \text{sec}}$$

where R is the distance to accelerator in meters. Thus, since the currents and also the U. V. emission lasts for approximately 10^{-6} sec, the ionization fraction is the order of 5% at 1 meter from the source and 100% at 20 cm.

This calculation indicates the following: (1) close to the accelerator ($\sim$ 20 cm) the ambient gas is fully ionized and the pickup mechanism must be similar to Longmire's model,[2] (2) further from the accelerator ($\sim$ 1m) the gas is 95% neutral and the pickup mechanism must be associated with charge exchange and ionizing collisions in the presence of a magnetic field.

In regard to the second conclusions, we note that the cross section for charge exchange and direct ionization collisions are of the order 10^{-15} cm^2 for ion energies of the order 1.5 kev. The mean free path for these processes at 10μ is $\sim$ 3 cm which is much smaller than the flow scale. The mean free path for ordinary momentum transfer collisions is larger than the flow scale (3 meters).

Optical Data

Two optical instruments were used in this experiment: a high speed image converter camera and a set of rotating mirror cameras. Snapshots at the accelerator taken with the image converter camera are shown in Fig. 4. The timing and exposure of the camera placed at the rear wall of the tank facing the accelerator were adjusted to view the initial stages of breakdown. The exposure time of 50 nanoseconds is sufficiently rapid to resolve asymmetries on the scale of 1 cm (assuming velocities of 10^7 cm/sec). From the photographs in Fig. 4, it appears that (1) the annular region of the accelerator is filled with luminous plasma as early as $1/2 \mu$ after initiation of the current pulse and (2) no gross (azimuthal) asymmetries are present near the peak of the current cycle ($\sim 1 \mu$ sec).

In addition, measurements were made of the convected magnetic field in the plasma at large distances from the source (up to 1 meter). These measurements were made at various azimuthal locations and no gross asymmetries were found when the accelerator was loaded with four symmetrically placed wires.

HEAD ON VIEW OF ACCELERATOR
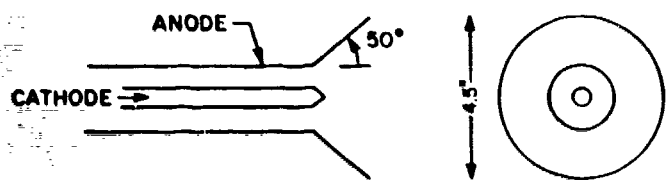
EXPOSURE – 50 NANOSECONDS

Fig. 4   Head On View of Accelerator

-14-

B2493

Typical data from the rotating mirror cameras are shown in Fig. 5. These are x-t diagrams of the luminous front taken at a background pressure of 45 μ with and without an applied axial field. These results show, with striking clarity, the fundamental result of this experiment: the aluminum plasma is considerably decelerated when a magnetic field is applied albeit the direction of the field is parallel to its motion. It must be emphasized that this phenomenon is observed even when the energy of the plasma is very large compared to the energy of the ambient magnetic field, (see next section). This means that the ambient magnetic field can play no direct role in appreciably decelerating the plasma, but can only act as an intermediary in the momentum transfer process resulting from charge exchange and direction ionization collisions.

A summary of the mirror camera data taken at 45 μ is shown in Fig. 6. At pressures above 100 μ, the aluminum plasma starts to pick up the ambient gas by ordinary momentum transfer collisions and therefore 50 μ was the highest pressure for which the effects of charge exchange and ionizing collisions alone were studied.

The data in Fig. 6 shows position versus time of the luminous front for four different applied magnetic field intensities. It must be pointed out that the aluminum ion plasma does have an azimuthal component of B field which appears to be convected with it, whether or not there is an applied axial bias field. Figure 7 shows the magnitude of this field as a function of time for no applied field. The deceleration of the aluminum plasma (debris) appears to be a function of the magnitude of the applied axial magnetic field until the field intensity is equal to 200 gauss. At 200 gauss the gyro radius of an air ion is either 50 cm (at $\omega t = 14$) or 100 cm (at $\omega t = 28$) when the ion speed is equal to the initial debris velocity. The experimental results indicate that a further increase in B field or flow dimension would not affect the debris motion.

The data on Fig. 7 for $B_z = 0$ shows some deceleration, which is possibly due to two effects.

The first deals with the manner in which the detector (camera) records the position of the leading edge of the luminous front and this is discussed in the Appendix. The analysis in the Appendix is for an ideal gas expanding in a vacuum. It is shown that if an instrument such as a camera records the position of a threshold level of light intensity vs time, its trajectory always appears to decelerate.

The second effect causing deceleration is that even with no applied field, the residual magnetic field locked in the plasma primarily in the azimuthal direction and therefore perpendicular to the motion. Charge exchange and ionizing collisions can couple momentum to the aluminum plasma via this azimuthal field causing the plasma to decelerate a small amount even in the absence of an applied axial field.

The deceleration of the plasma as a function of pressure for constant applied axial magnetic field ($\sim$ 200 gauss) is shown in Fig. 8.
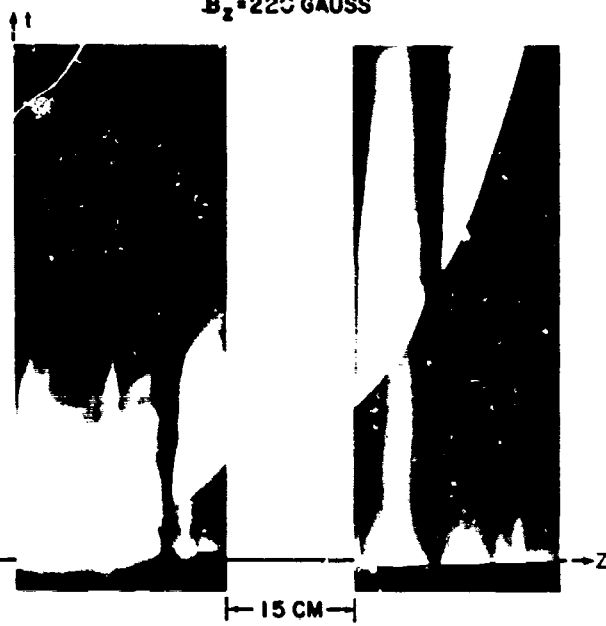
-15-
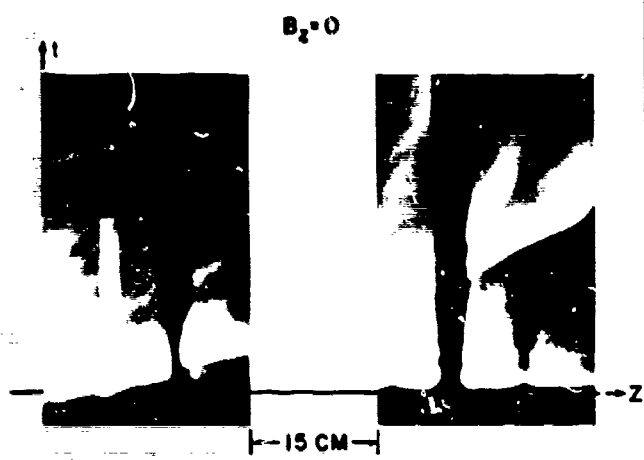
Fig. 5   Mirror Camera Data

B2489
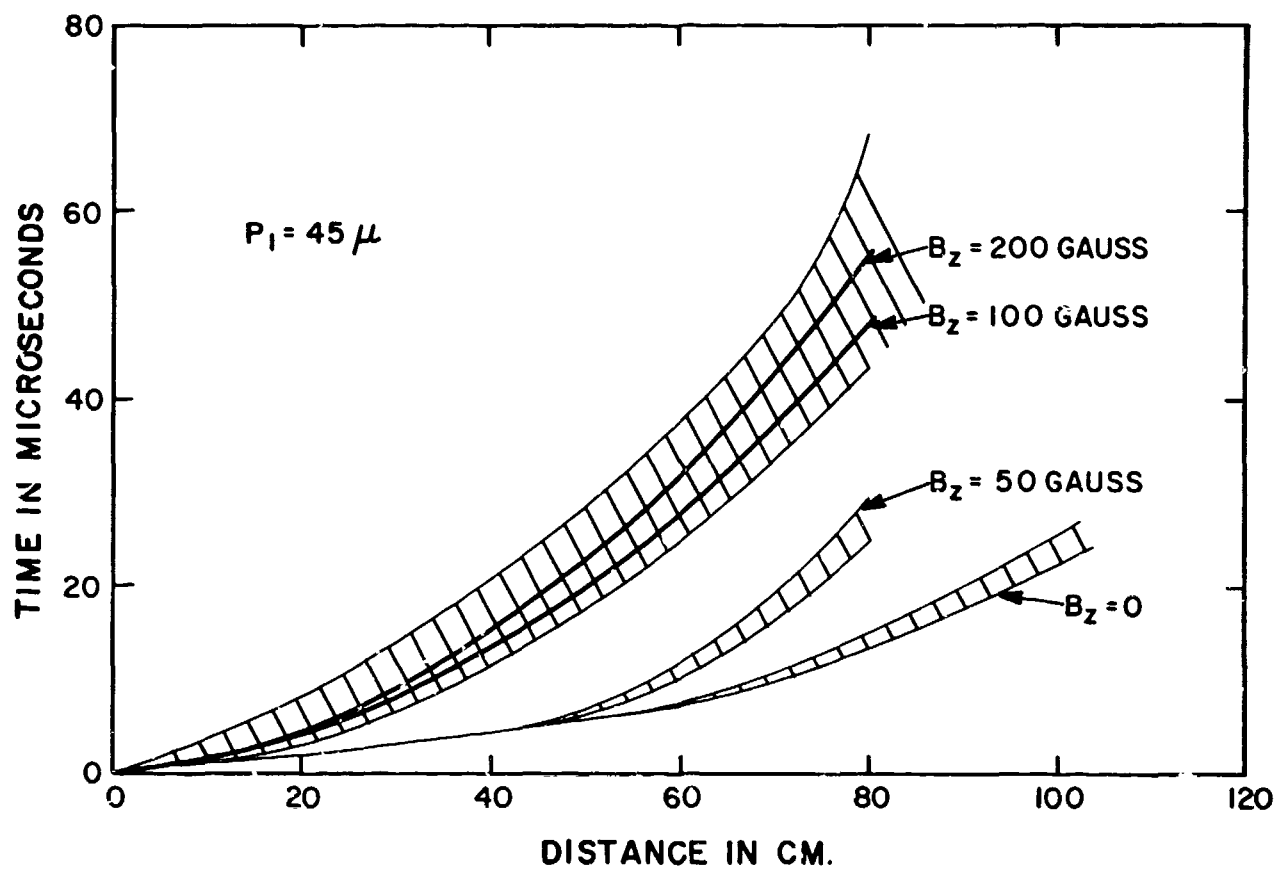
Fig. 6   Aluminum Plasma Motion vs Time with Applied Field as
Parameter

B2488
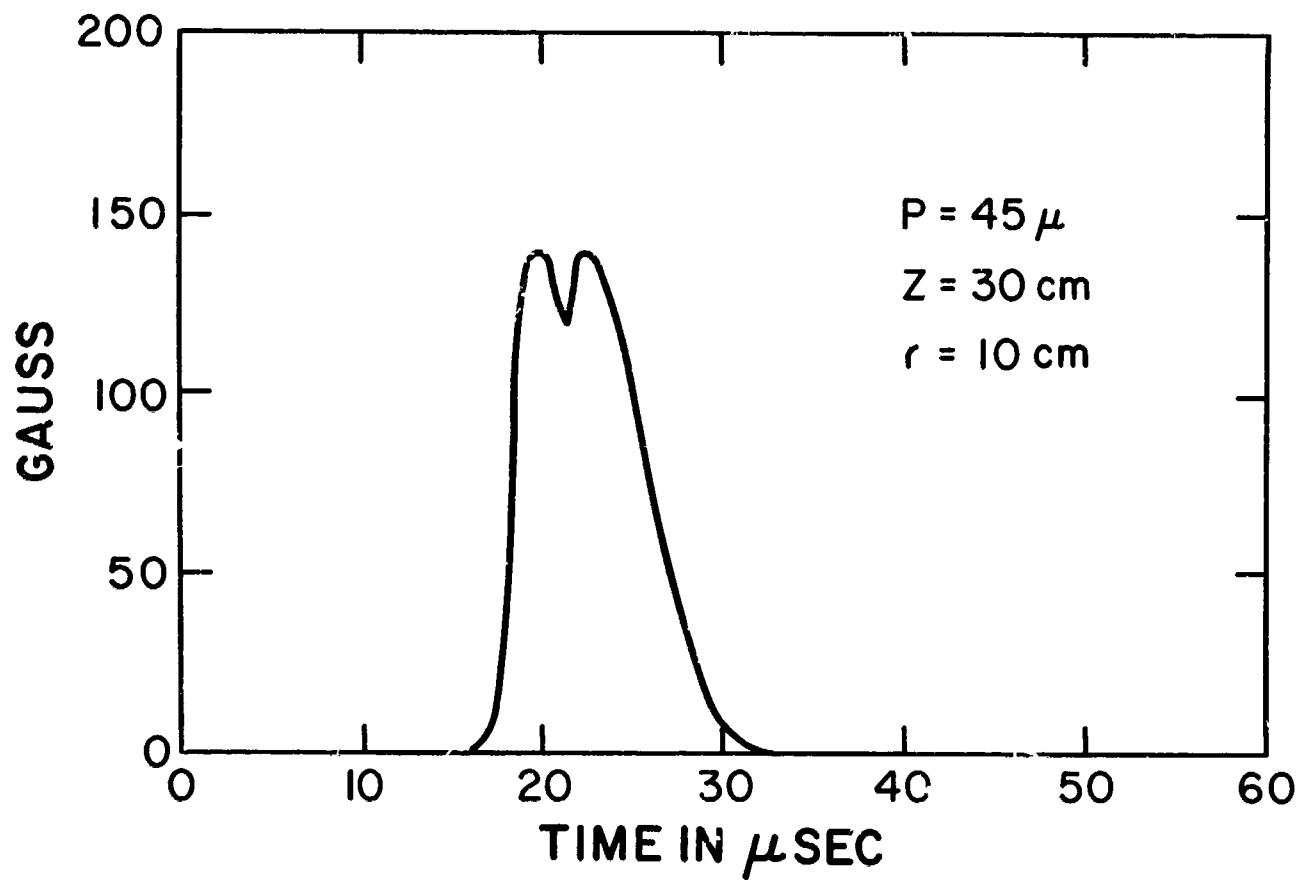
Fig. 7   Azimuthal Magnetic Field with no Applied Axial Field

B2569

SOLID LINES:

$$v(t) = \frac{v_0}{1 + \frac{1}{m_0}\frac{\pi}{3}\alpha^2 Z^3 \rho_0}$$

$P_1 = 45\mu$
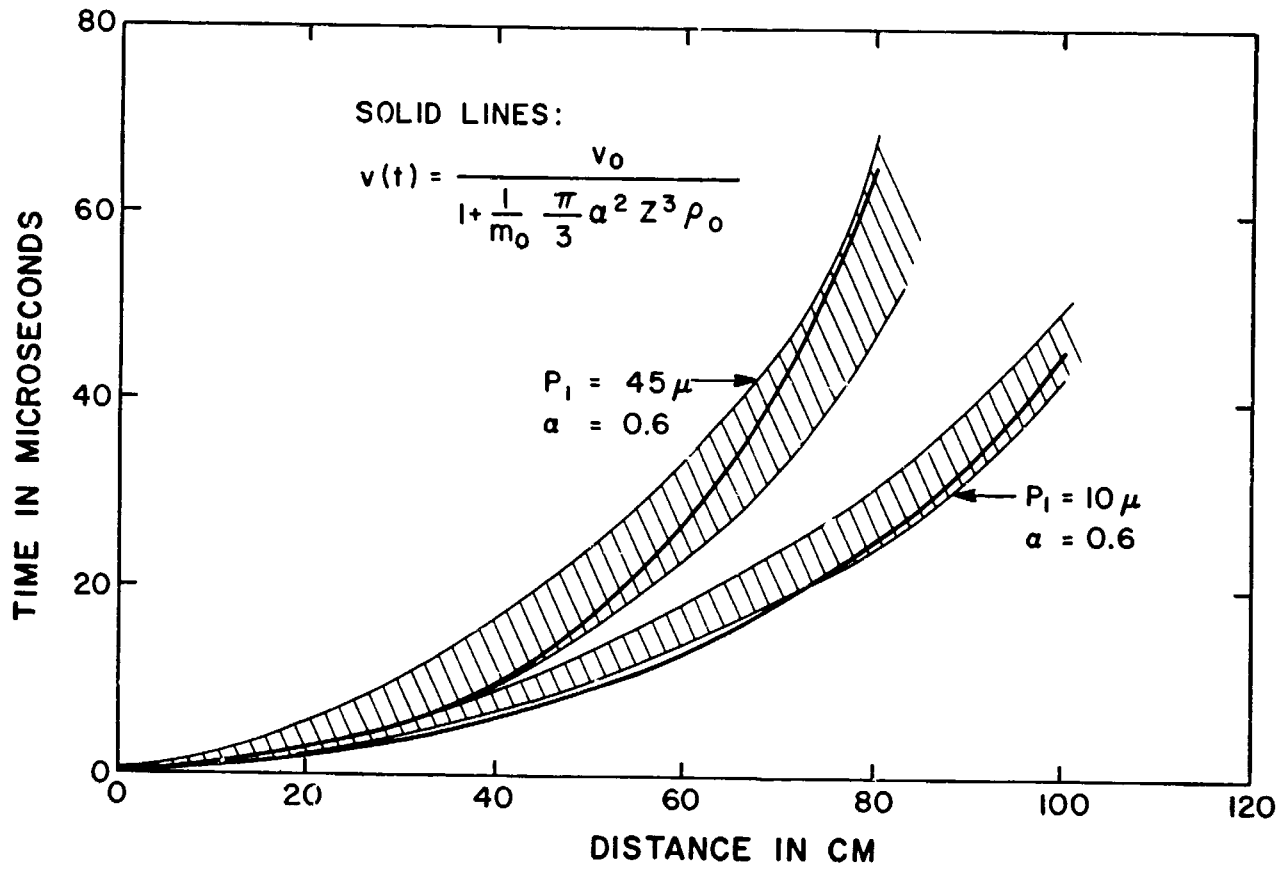$\alpha = 0.6$

$P_1 = 10\mu$
$\alpha = 0.6$

Fig. 8   Aluminum Plasma Motion at Center Line vs Time with Axial B Field

-19-

B2481

For comparison, x vs t has been plotted assuming simple momentum conservation (snow plow model - Eq. (8)). The only differences between this model and that of Eq. (8) is that the neutral gas is swept up by charge exchange and ionizing collisions in the presence of a magnetic field (instead of ordinary collisions). To obtain the best fit with the data, a cone with radius to height ratio, $a = 0.6$ was used, although the results are not sensitive to the choice. Magnetic field data presented in the next section confirms this geometry.

Mirror camera data was also obtained at $15\,\mu$ and at $2\,\mu$. These results appear to scale with the same pressure dependence as shown in Fig. 8.

IV. MAGNETIC FIELD DATA

Magnetic field probes were used first to confirm the velocities measured by the mirror cameras and second to determine the geometry and magnitude of the magnetic field. These probes were placed at different axial locations to measure the velocity of the magnetic disturbances. In these first tests, no axial field was applied, so the only field present was that associated with the plasma. The results of these tests can be summarized as follows:

1. A sharply defined B_θ (see Fig. 7), pulse was observed with no radial, Br or axial, B_z signals.

2. The absolute space-time position of these B_θ pulses roughly correspond to the mirror camera data.

3. The time difference between the B_θ signal for various axial stations coincided with mirror camera data.

4. The magnitude of the B_θ field scales roughly as $z^{-3/2}$. This fact indicates that the magnetic energy locked in the aluminum plasma is constant and the magnetic energy density merely decreases as the volume of the bubble increases.

5. The magnetic energy associated with the B_θ field is many orders of magnitude less than the kinetic energy of the plasma. The value for B_θ is usually less than 100 gauss, which when evenly distributed over a volume 30 cm on a side only represents a total magnetic energy of $(B^2/2 \mu_o)$ (volume) $\simeq 10^{-1}$ joules. The initial kinetic energy of the aluminum plasma is $1/2 \, mv_o^2 \simeq 2 \times 10^3$ joules. The ratio of kinetic to magnetic energy = 2×10^4. This indicates that after a relatively small expansion, the accelerator has produced a plasma with only kinetic energy, i.e., there is very little magnetic field pushing the plasma. Consequently, the currents in the plasma are relatively small and in this respect the plasma simulates nuclear debris.

The remainder of the magnetic field data was taken with an applied axial magnetic field (50-220 gauss) in order to measure the perturbation in the ambient field. Examples of the B field data taken 60 cm from the accelerator at radii of 10 cm and 40 cm are shown in Figs. 9 and 10 and Fig. 11 respectively.

Qualitatively, the dynamics of the magnetic field bubble are as follows: The moving plasma pushes the ambient axial field out of the way and creates a field free region. After the plasma passes, the field closes
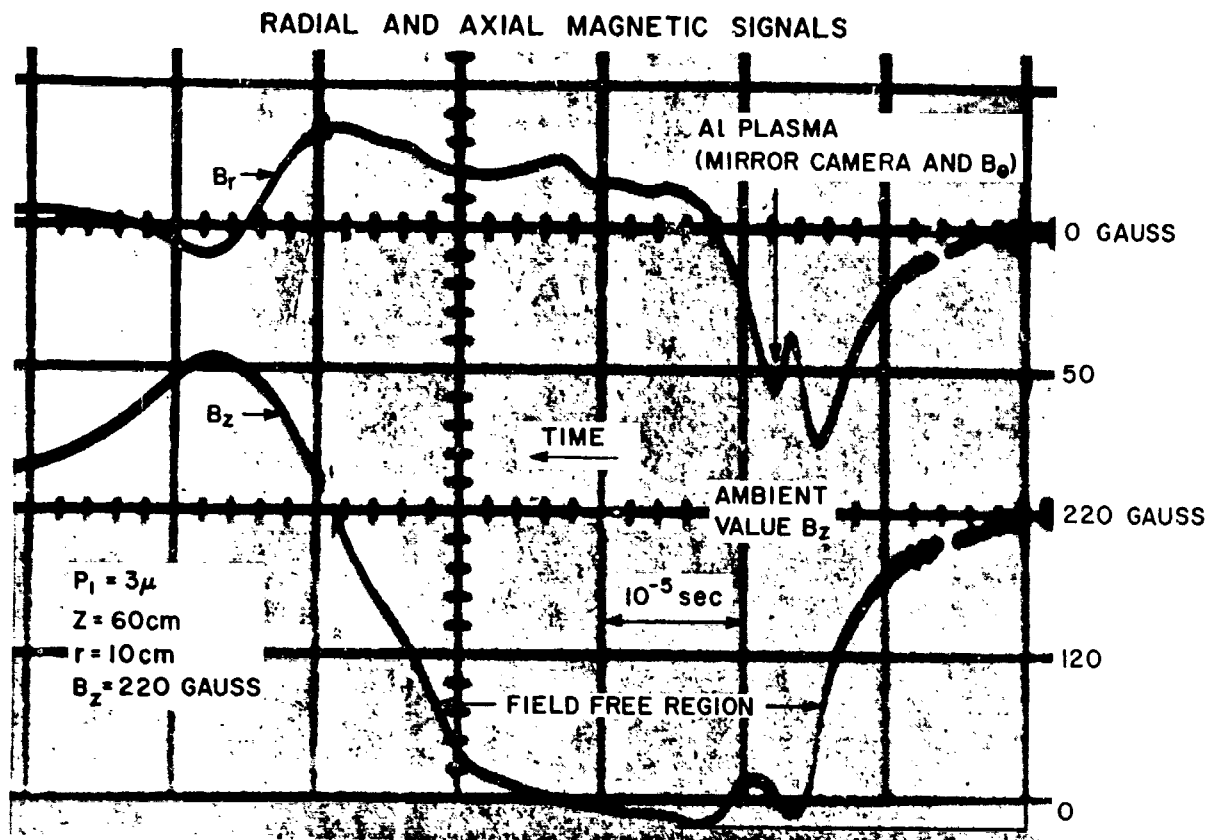
RADIAL AND AXIAL MAGNETIC SIGNALS

Fig. 9   Radial and Axial Magnetic Signals (z = 60 cm, R = 10 cm)
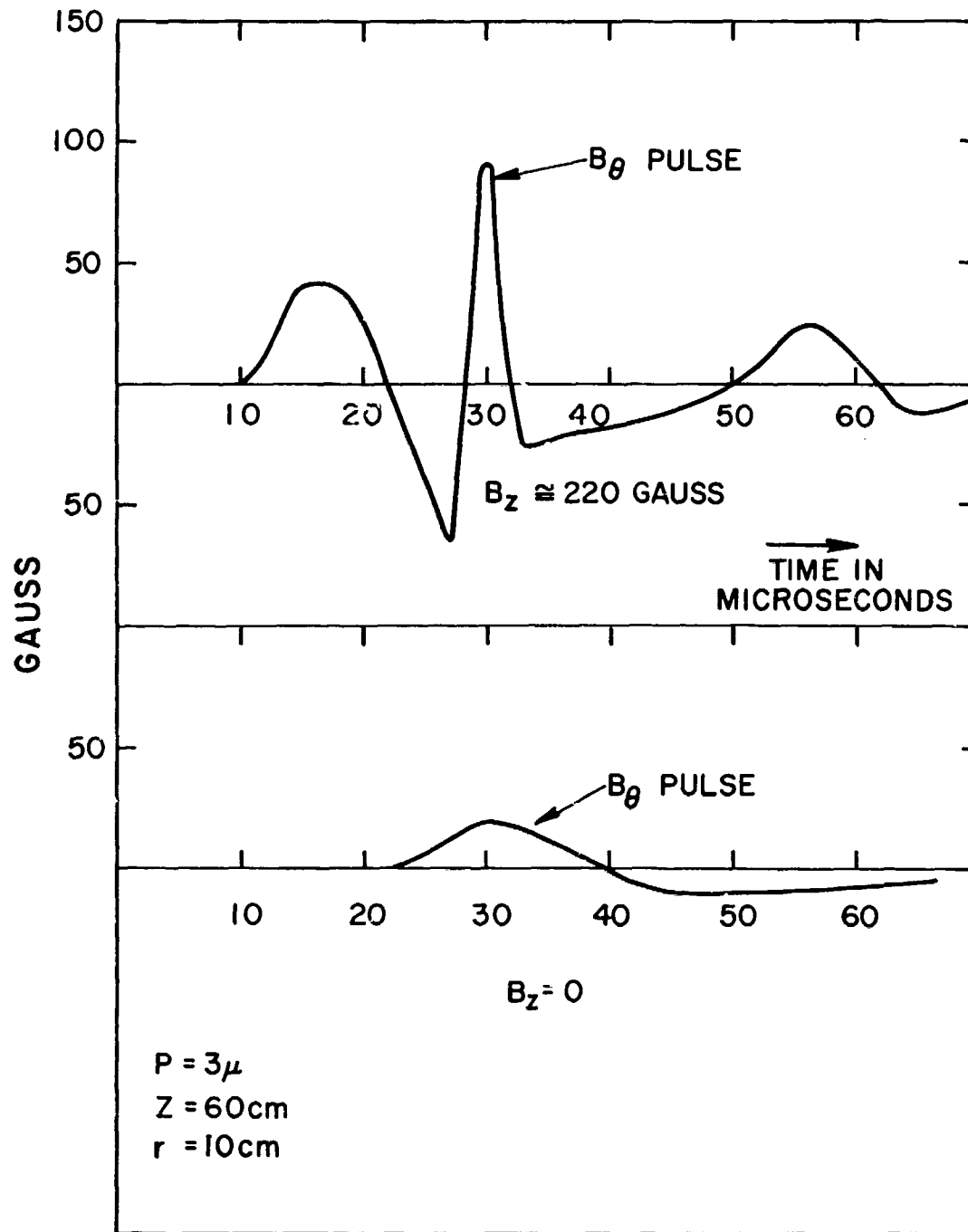
B2494

Fig. 10   Azimuthal Magnetic Field Signals (z = 60 cm, R = 10 cm)
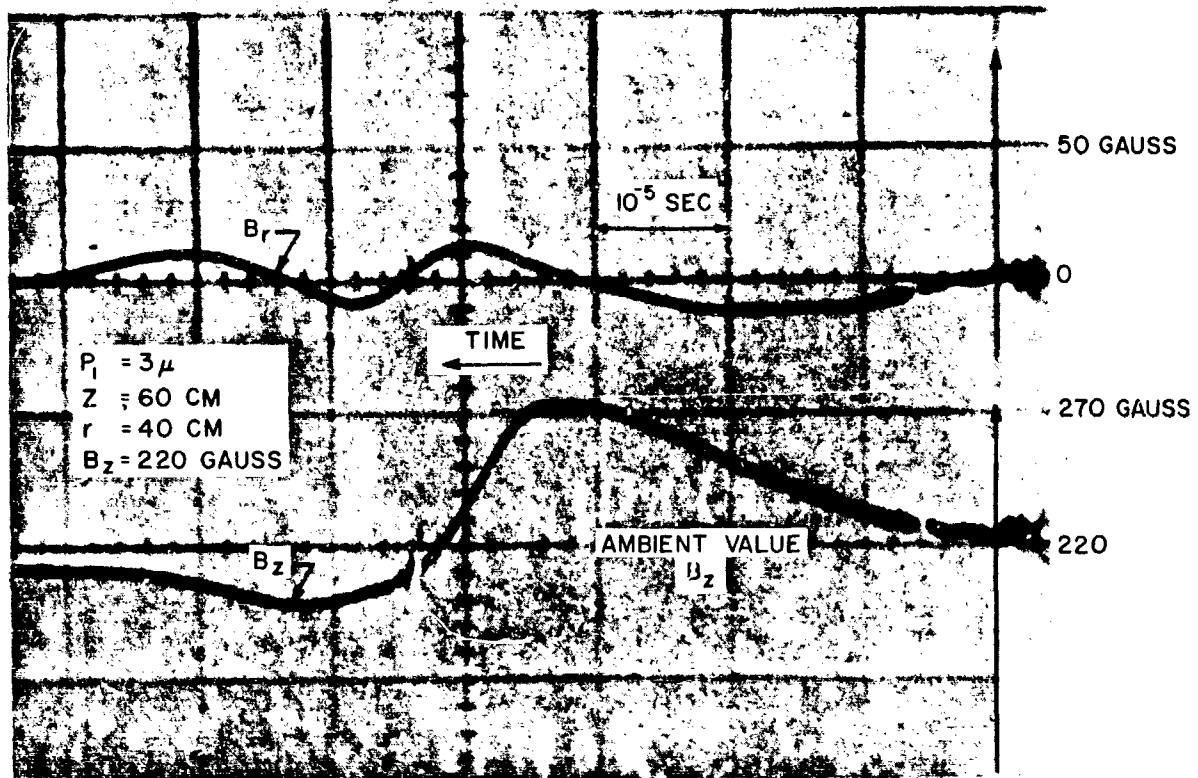
-23-

RADIAL AND AXIAL MAGNETIC SIGNALS

Fig. 11   Radial and Axial Magnetic Signals (z = 60 cm,   R = 40 cm)

B2495

behind. A composite picture of the magnetic field bubble is shown in Fig. 12. The bubble is approximately 40 cm in radius and this agrees with the assumption of $\alpha \simeq 0.6$ as shown in Fig. 8. This picture was drawn from data taken at one axial location (60 cm) and at several radial positions and "unfolded" in space using a constant velocity (2.5 cm/μ sec) obtained from mirror camera data.

There are a number of important features shown in Fig. 9 and 10. They are:

1. The rise time of the leading edge of the bubble is ~ 8 μ sec which at a velocity of 2.5 cm/μ sec corresponds to a thickness of ~ 20 cm. The gyroradius of an aluminum ion traveling at this speed in a field of 220 gauss is 28 cm and thus the thickness would appear to be comparable to an ion gyro radius. If, instead, we assume that at 60 cm, the aluminum plasma has a large amount of swept up air within it, the average ion mass could be lowered (atomic weight of dissociated air ~ 14 as compared to ~ 27 for aluminum).

2. The ambient axial field is completely excluded for approximately 50 cm.

3. There exists a spike in both radial and axial field signals which corresponds exactly to the time that the azimuthal field which is recorded at the same axial location, (see Figs. 9 and 10) has a sharp increase. The magnitude of the azimuthal field is approximately equal to 150 gauss (when there is an applied axial field) while the spike in the radial and axial field traces is only 25 gauss.

The existence of the disturbance in the ambient axial field for a distance approximately equal to an ion gyro radius ahead of the aluminum plasma could indicate an MHD shock (collisionless) in the ambient B field and plasma. This has not yet been verified but remains as an interesting point for further study.

4. At late times in Fig. 9, the axial field trace shows slight enhancement as the ambient field recloses around the plasma.

5. In Fig. 11, at a larger radial position, we note that the axial field is initially enhanced before it relaxes back to its original state. This effect is caused by the bunching up of the axial magnetic field lines at the edge of the bubble (see Fig. 12). We note that in this high velocity flow (high speed w.r.t. the ambient Alfven speed) the wake should appear hypersonic and should be almost flat against the plasma itself. The lines of force crowd together at the edge and the radial disturbance does not extend far from the plasma.

Magnetic field data at this same pressure (2 μ) but at lower values of ambient field show that this picture is unchanged. At higher pressures, $10\,\mu$ - $45\,\mu$, it is found that the plasma still excludes the ambient field over a significant volume but this only occurs closer to the accelerator, i.e.,

-25-
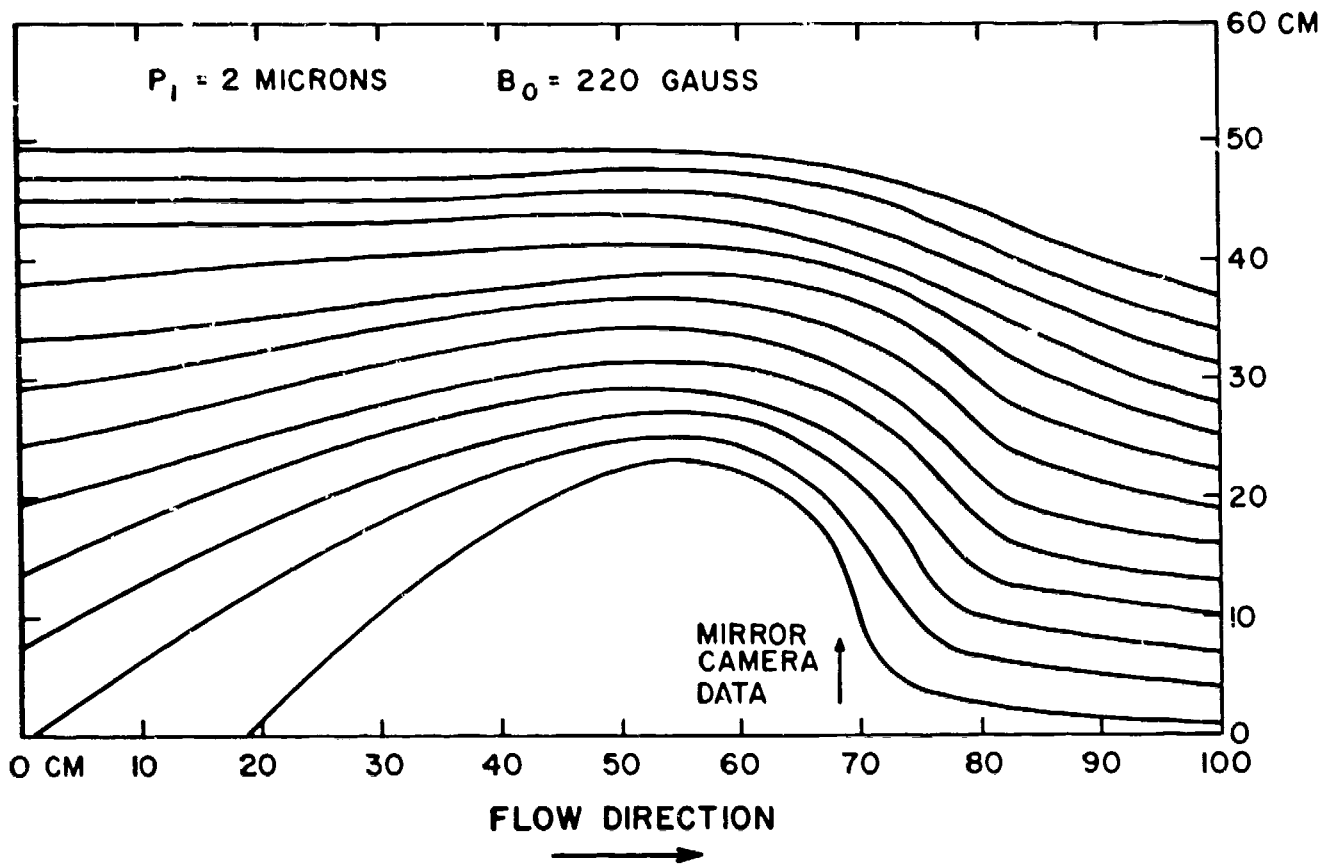
Fig. 12   Magnetic Field Profile

B2579

before the plasma is greatly decelerated. At the observation station of z = 60 cm, R = 10 cm, 75% of the ambient field is excluded at 10μ and 50% at 45μ.

There is also a qualitative difference in the high pressure data. The data is less reproducible and has more fluctuations than at the lower pressures. It is possible that at higher pressures, the strong rate of deceleration caused instabilities (e.g., Taylor instabilities) which might account for the erratic data. It is interesting to point out that this experimental facility might be useful in the simulation of late time debris motion when the magnetic field is collapsing back into the bubble.

V. CONCLUSIONS

This experiment has demonstrated that a magnetic field is important in the momentum balance of the moving aluminum plasma even though (1) the magnetic field energy is insignificant when compared to the plasma kinetic energy and (2) the ambient magnetic field is parallel to the flow velocity. The way in which the magnetic field decelerates the plasma is to provide a momentum coupling for charge exchange and direct ionization collisions.

Several aspects of high altitude nuclear explosions have been simulated by this experiment including preionization of the ambient air, a high velocity plasma with a very small convected magnetic field and an essentially planar front parallel to the ambient field. By no means have we attempted to simulate the entire picture of high altitude nuclear explosions, but only to confirm certain assumptions of the model advanced by Workman.[3] To that end, we have confirmed that the moving plasma turns the ambient (axial) field until it lies within the plane of the bubble and that a field free region is created. Moreover, the streak camera photographs show that the aluminum plasma gives up momentum to nearly all of the partially ionized air that it passes over when the ambient axial B field intensity just large enough (200 gauss) to make the air ion gyro radius comparable to the flow dimensions (50-100 cm). At lower B field intensities, the coupling appears to be only partial.

There are many details of the flow configuration which although not essential to the Workman's model, are interesting in the sense of plasma physic research. It appears from the magnetic field data, that the ambient magnetic field is turned ahead of the aluminum plasma region and that the thickness of this transition region is of the order of an ion gyro radius. Also, the magnetic field traces show structure (e.g., the spike of azimuthal field associated with the plasma) which is much smaller than an ion gyro radius indicating that perhaps there is yet a smaller relevant scale length. Finally this form of plasma accelerator has proven to be a reliable, well calibrated tool for high velocity plasma research and a simple method has been demonstrated by which a known amount of material can be vaporized, ionized and accelerated reproducibly. Since only one half the capacitor bank voltage was used for these experiments, it should be possible to raise the exhaust velocity to perhaps $\sim 2 \times 10^7$ cm/sec and this will be done in the near future.

Although we know that a deceleration mechanism for debris along field lines does exist, the second prediction of Workman concerning the charge exchange leak has yet to be investigated. Confirmation of this charge exchange leak is one of our remaining goals.

APPENDIX

LOW PRESSURE EXPANSION

As indicated in Fig. 6, the aluminum plasma decelerates even with no applied field. In Fig. 13, data is shown for no applied field at 15 μ and 45 μ. Aside from the observation that both curves show deceleration, the lower pressure data shows a higher rate of deceleration than the high pressure data. These two phenomena can be explained in a qualitative sense by examining the characteristics of the detector (photographic film).

Film requires a minimum or threshold value of light intensity, I_d, to visibly record an event. I_d is a function of the aluminum plasma density, n, and the specific functional dependence is related to the specific radiation process which is responsible for the light emission. In any case, I_d corresponds to aluminum density, n_d, and it is the trajectory of n_d which is shown in the mirror camera photographs.

As a model for the calculation of this trajectory, consider that at time $t = 0$, at $z = 0$, the aluminum plasma is suddenly given the one dimensional velocity distribution as shown in Fig. 14.

$$f(v, t=0, z=0) = \frac{No}{\sqrt{2\pi}\, a_o} \, e^{-\frac{1}{2 a_o^2} (v-v_o)^2} \tag{A1}$$

where No = total number of aluminum particles

$$a_o = \sqrt{kT_o/m_o} = \text{initial sound speed}$$

$$v = z \text{ component of velocity}$$

$$v_o = \text{initial velocity}$$

Assuming that the plasma flows into a field free, vacuum region and that the plasma particles do not interact with each other, the density distribution as a function of (z, t) will be

$$n(z, t) = \frac{No}{\sqrt{2\pi}\, a_o} \, \frac{1}{t} \, e^{-\frac{1}{2 a_o^2 t^2} (z-v_o t)^2} \tag{A2}$$

-31-
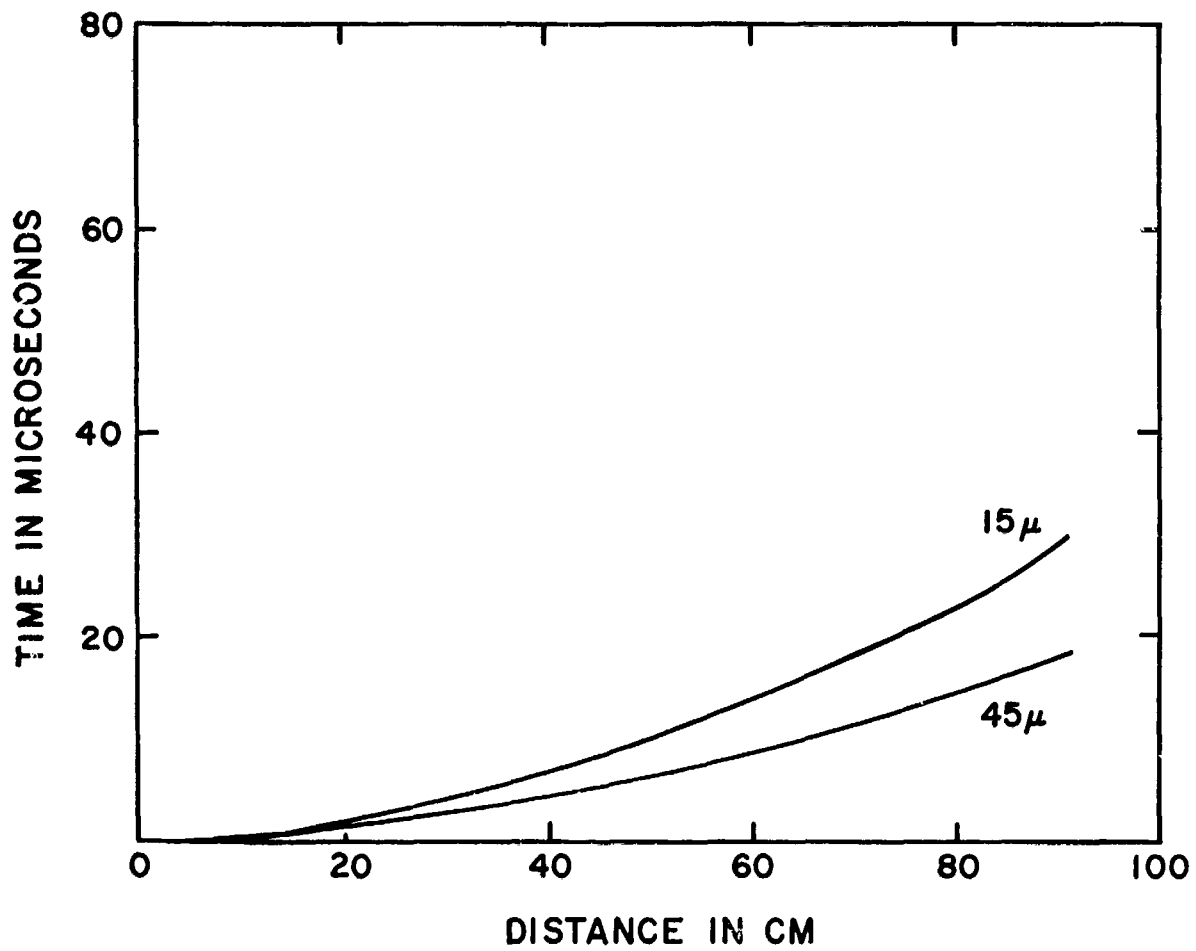
Fig. 13   Aluminum Plasma Motion vs Time with no Applied Field and
Pressure as a Parameter

$f(v, z = 0, t = 0)$

INITIAL DISTRIBUTION

$$\tau = \frac{N_0 / n_d}{\sqrt{2\pi}\, a_0}$$
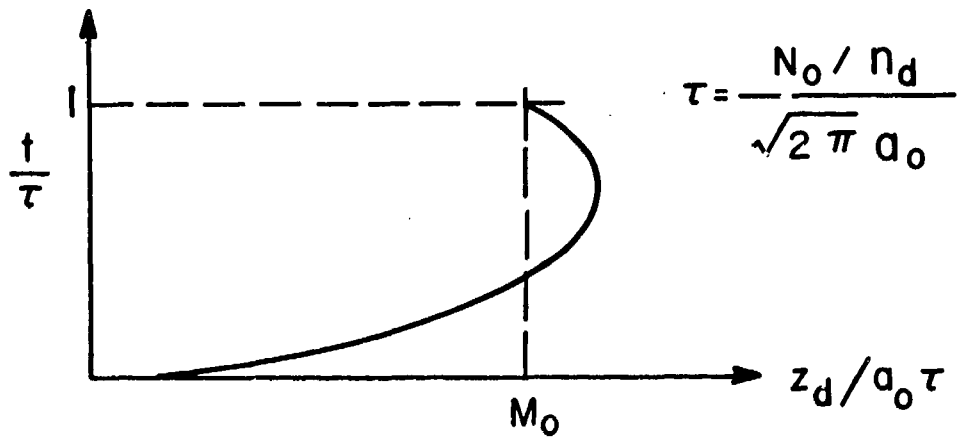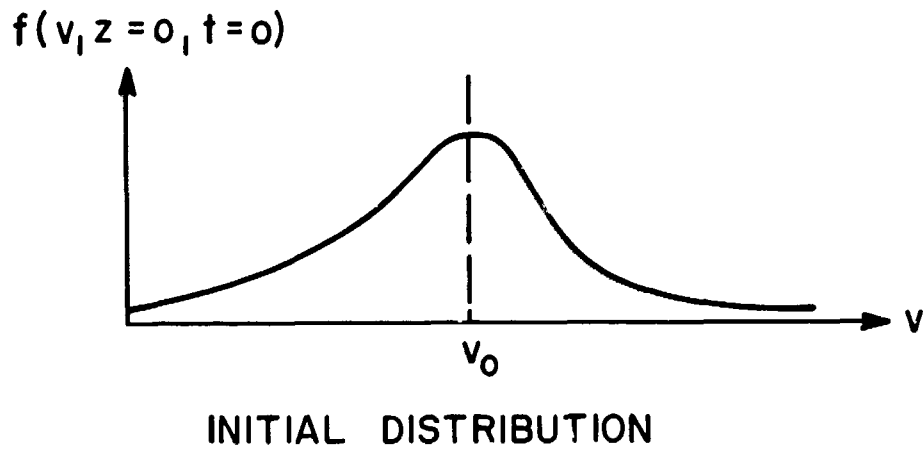
TRAJECTORY OF THRESHOLD IN FILM INTENSITY

Fig. 14   Vacuum Deceleration

-33-

A three dimensional expansion would only change power of t in the coefficient of the exponential from one to three, and the qualitative results would be identical. Denoting by z_d, the point which corresponds to the threshold density, n_d, the trajectory of this point is given by

$$z_d(t) = v_o t \left[1 + m_o^{-1} 2 \log \tau/t\right] \tag{A3}$$

where $m_o = v_o/a_o$

$$\tau = \frac{No}{n_d} \frac{1}{\sqrt{2\pi} \, a_o}$$

A sketch of $z_d(t)$ is shown in Fig. 14 and it is clear from the curvature that the acceleration is always negative. Furthermore, if the vacuum region is replaced by a low pressure background, a typical pressure dependence for n_d would be

$$n_d \propto P^\beta \; ; \; \beta < 0$$

so that

$$\log \tau/t \propto \log P$$

It can then be shown that the acceleration of $z_d(t)$ varies as

$$\frac{d^2 z_d}{dt^2} \propto \frac{1 + \frac{1}{\text{Log } P}}{\sqrt{\text{Log } P}} \tag{A4}$$

Thus, on the basis of this low pressure expansion into a given threshold intensity level for film, (1) zero field expansions should decelerate more than into those of higher pressure.

As previously stated, there is always a residual magnetic field locked into the plasma so that this vacuum deceleration mechanism is never singly present in this experiment. However, its effect in this experiment, as well as in any optical measurement of high altitude nuclear explosions, must be recognized.

REFERENCES

1. Walker, W. C., Wainfan, N., Weissler, G. L., J. Appl. Phys. 26, (1955) 1366.

2. Longmire, C. L., "Notes on Debris-Air-Magnetic-Interaction," Memo RM-3386-PR, January 1963, The Rand Corporation.

3. Workman, J., "Debris Expansion Model," (SECRET), presented at Conference on Nuclear Weapons Phenomena, Sandia Base, New Mexico, June 1968.

BLANK PAGE

DISTRIBUTION LIST FOR CONTRACT DASA01-67-C-0131

Director, Advanced Research Projects Agency, Washington, D.C. 20301 Attn: NTPO (1 copy)
Technical Information Officer (1 copy)
Radar and Optical Technology (1 copy)
PA branch (1 copy)
Dr. R. C. Brouns (1 copy)
Captain W. T. Boyer (1 copy)
LTC R. M. Dowe (1 copy)
Dr. Dave Mann (Defender) (1 copy)
Sto. (Strategic Tech. Office.) (1 copy)
Dr. J. Wade (1 copy)

Director, Armed Forces Inst. of Pathology, Walter Reed Army Medical Center, 14th Street and Alaska Avenue, Washington, D.C. 20305 (1 copy)

Commandant, Armed Forces Staff College, Norfolk, Virginia 23511 Attn: Library (1 copy)

Chairman, Armed Services Explosives Safety Board, NASSIF Building, Washington, D.C. 20315 Attn: Mr. R. G. Perkins (1 copy)

Director, Defense Atomic Support Agency, Washington, D.C. 20305 Attn: Dr. N. F. Wikner (DDST) (1 copy)
Dr. J. Young (DDST) (1 copy)
STRA (1 copy)
RAAE Ltc. Fitz (2 copies)
RARP (1 copy)
RAEV (1 copy)
STAP (1 copy)
STSP (1 copy)
SPLN (1 copy)
Technical Library (APTL) (2 copies)
SPSS (1 copy)
SFAS (1 copy)
STMD (1 copy)
OAOP (1 copy)

Director, Defense Atomic Support Agency, Armed Forces Radiobiology Research Inst., National Naval Medical Center, Bethesda, Maryland 20014
Attn: Security Officer (1 copy)
PSD (1 copy)
RPD (1 copy)
BSD (1 copy)

Chief, Joint Atomic Information Exchange Group, Washington, D.C. 20305 (1 copy)

Commander, Field Command, Defense Atomic Support Agency, Sandia Base, Albuquerque, New Mexico 87115 Attn: Document Library (1 copy)
FCDV (1 copy)
FCDV-1 (1 copy)
Code 540, J. A. Krcek (1 copy)
C.W. Herr, Code H820 (1 copy)
Asst. Dir., D&O/Col. La Franz,
Code 530 (1 copy)

Administrator, Defense Documentation Center, Cameron Station - Bldg. 5, Alexandria, Virginia 22314 Attn: Document Control (20 copies)

Director, Defense Intelligence Agency, Washington, D. C. 20301 Attn: DIAAP-8B (1 copy)
Mrs. Meades (1 copy)
DIAAP, Mr. O'Farrell (1 copy)
DIAST-5 (1 copy)
DIAAP-8b, R. C. Wise (1 copy)
DIAST-2c (1 copy)
DIAST-3 (1 copy)

Commandant, Industrial College of the Armed Forces, Ft. McNair, Washington, D.C. 20135 Attn: Document Control (1 copy)

Chief, Natl., Mil. Command System Support Ctr., Washington, D. C. 20301 Attn: Technical Library (1 copy)

Commandant, National War College, Fort Lesley J. Mc Nair, Washington, D. C. 20315 Attn: Class Rec. Library (1 copy)

U. S. Documents Officer, Office of the U.S. National Military Rep., APO New York 09055 Attn: Document Control (1 copy)

Assistant to the Secretary of Defense, (Atomic Energy), Washington, D.C. 20301 Attn: Document Control (1 copy)

Director of Defense Research and Engineering, Washington, D. C. 20301 Attn: Deputy Director (Strategic and Space Systems) (1 copy)
Asst. Director (Strategic Weapons) (1 copy)
Asst. Director (Nuclear Programs) (1 copy)
Asst. Director (Command and Control) (1 copy)
Asst. Director (Research) (1 copy)
Asst. Director (Communications and Electronics) (1 copy)
Asst. Director (Defensive Systems) (1 copy)

Director, National Security Agency, Ft. George G. Meade, Maryland 20755 Attn: A72 (1 copy)
S3 (1 copy)
C3/TDL (1 copy)
David Sloan (1 copy)
Neal Carson (1 copy)
D42, T. Spencer (1 copy)
Technical Library (1 copy)

Director, Weapons Systems Evaluation Group, Washington, D. C. 20305 Attn: Library/Col. Holden (1 copy)
Dr. Gerald Rosen (1 copy)
Dr. H. A. Knapp (1 copy)

Joint Chiefs of Staff, Department of the Army, Olney, Maryland 20832 Attn: Kirk Fox, Director (1 copy)
Mr. Baker (1 copy)
Ops. Res. Div., Robert S. Triplett (1 copy)

Assistant Chief of Staff, Army Communications-Electronics, Department of the Army, Washington, D.C. 20315 Attn: Code (DCC-E) (1 copy)
CCEFM-5B1 (1 copy)

Chief of Engineers, Department of the Army, Washington, D.C. 20315 Attn: ENGMC-EM (1 copy)
ENGTE-E (1 copy)

Asst. Chief of Staff for Force Development, Department of the Army, Washington, D. C. 20310 Attn: Directorate of CBR & Nuclear Ops. (1 copy)

Asst. Chief of Staff for Intelligence, Department of the Army, Washington, D. C. 20310 Attn: Document Control (1 copy)

Deputy Chief of Staff for Military Ops., Department of the Army, Washington, D.C. 20310 Attn: Document Control (1 copy)

Chief of Research and Development, Department of the Army, Washington, D.C. 20310 Attn: Nike-X and Space Division (1 copy)
Advanced Ballistic Missile Defense Agency (1 copy)
Dr. J. B. Gilstein (Dir. -ABMDA) (1 copy)
Nuclear, Chemical-Biological Div. (1 copy)

Chief of Staff, Army Sentinel System Office, 206 N. Washington Street, Alexandria, Va. 22314 Attn: CSSSO (Plans Div.) (1 copy)

Surgeon-General, Department of the Army, 18th and Constitution Ave., N. W., Washington, D. C. 20315 Attn: MEDDH-N (1 copy)

Commanding Officer, Army Research Office, Life Sciences Division, 3045 Columbia Pike, Arlington, Va. 22204 Attn: Chief, Scientific Analysis Branch (1 copy)

Commanding General, Continental Army Command, Ft. Monroe, Va. 23351 Attn: ATUTR-TNG/NBC (1 copy)

Headquarters, U. S. Army- 1 St. Fort Geo. G. Meade, Maryland 20755 Attn: AHABD-BAC (1 copy)

Commander-In-Chief, U. S. Army Europe, APO New York 09403 Attn: ECJB-T (1 copy)
                                                                   ODCSOPS (1 copy)

Commander-In-Chief, Department of the Navy Attn: Mr. Ksanda (1 copy)
                                                  Mr. Cassidy (1 copy)
                                                  Mr. Zigman (1 copy)
                                                  L. G. Haggmark (1 copy)
                                                  Wm. H. Yundt (1 copy)
                                                  Code 222C (1 copy)

Director, Naval Research Laboratory, Washington, D. C. 20390 Attn: Equipment Research Branch-Code 5360 (1 copy)
                                                                   Code 2027 (1 copy)
                                                                   Classified Material Control Branch (1 copy)
                                                                   L. S. Birks (1 copy)
                                                                   Dr. C. Johnson (1 copy)
                                                                   Dr. R. M. Dewitt (1 copy)
                                                                   Dr. F. J. Campbell (1 copy)
                                                                   Dr. R. Statler (1 copy)
                                                                   Technical Library (1 copy)
                                                                   Dr. A. Kolb (1 copy)
                                                                   Dr. K. Haine (1 copy)
                                                                   Dr. William Faust (1 copy)

Commanding Officer, Naval Schools Command, Treasure Island, San Francisco, California 94130 Attn: NBCD Department (Technical Library) (1 copy)

Commanding Officer, Naval School, Civil Engineer Corps, Officers, Naval Construction Battalion Center, Port Hueneme, California 93041
                                                                   Attn: Librarian (1 copy)

Officer in Charge, Naval Scientific and Technical Intelligence Ctr., Naval Observatory, Department of the Air Force Attn: Technical Library (1 copy)

Alaskan Air Command, APO Seattle 98742 Attn: ALDOE-P (1 copy)

USAFE, APO New York 09633 Attn: Intelligence Research Center (IRCTA-W) (1 copy)

AF Aero-Propulsion Laboratory, AFSC, Wright-Patterson AFB, Ohio 45433 Attn: APE, Lt. Col. L. W. Tate (1 copy)

AF Armament Laboratory, AFSC, Eglin AFB, Florida 32542 Attn: ATBT, R. L. Mc Guire (1 copy)
                                                              ATWT, W. H. Dittrich (1 copy)

Air Force Avionics Laboratory, AFSC, Wright-Patterson AFB, Ohio 45433 Attn: M. P. Gauvey (1 copy)
                                                                            AVPT (STINFO Office) (1 copy)

AF Cambridge Research Laboratories, OAR, L. G. Hanscom Field, Bedford, Massachusetts 01730 Attn: Dr. K. S. W. Champion, Crub (1 copy)
                                                                                                  Crub, Mr. J. Ulwick (1 copy)
                                                                                                  CRT (1 copy)
                                                                                                  Dr. W. Pfister, Cruo (1 copy)
                                                                                                  CRF (1 copy)
                                                                                                  Dr. Newman, Cru (1 copy)
                                                                                                  Capt. L. R. Doan, Cror (1 copy)
                                                                                                  Dr. G. J. Gassmann, Crur (1 copy)
                                                                                                  CRMXLR, Research Library, Stop 29 (1 copy)
                                                                                                  CRFC, Mr. L. Katz (1 copy)
                                                                                                  CRFG (1 copy)
                                                                                                  CRFR (1 copy)
                                                                                                  CRN, Dr. John N. Howard (1 copy)
                                                                                                  CRUB, Dr. John Paulson (1 copy)
                                                                                                  CRW, Mr. Barrett (1 copy)
                                                                                                  CRWD, Mr. A. Kahan (1 copy)
                                                                                                  CRUQ (1 copy)
                                                                                                  CRWG, Mr. R. Dolan (1 copy)
                                                                                                  CRWH, Mr. E. Burke (1 copy)
                                                                                                  CROR, Mr. H. Gauvin (1 copy)
                                                                                                  CRUR, Mr. R. Cormier (1 copy)
                                                                                                  CRTE (1 copy)
                                                                                                  CROR (1 copy)
                                                                                                  Dr. R. E. Huffman, CRUS (1 copy)
                                                                                                  CRO (1 copy)

AF Communications Service, Scott AFB, Illinois 62225 (1 copy)

AF Director of Nuclear Safety, Kirtland AFB, New Mexico 87117 Attn: Document Control For AFINSR (1 copy)

AF Eastern Test Range, AFSC, Patrick AFB, Florida 32925 Attn: ETLG-1 (STINFO Officer) (1 copy)

AF Flight Dynamics Laboratory, AFSC, Wright-Patterson AFB, Ohio 45433 Attn: FDTR (1 copy)
                                                                            FDTR For Mr. F. Adams (1 copy)
                                                                            FDP, R. S. Hoff, Jr. (1 copy)

AF Flight Test Center, AFSC, Edwards AFB, California 93523 Attn: FTOP, Lt. Col. C. A. Garrett (1 copy)

AF Institute of Technology, AU, Wright-Patterson AFB, Ohio 45433 Attn: Dr. C. Bridgman/Bldg. 640, Rm 106 (1 copy)

AF Weapons Laboratory, AFSC, Kirtland AFB, New Mexico 87117 Attn: WLIL, Technical Library (1 copy)
                                                                   WLRET (Tree Group Leader) (1 copy)
                                                                   WLRTH, Maj. William Whitaker (1 copy)
                                                                   WLDE, (Electronics Br., Chief) (1 copy)
                                                                   Chief, WLDC (Civil Erg. Br.) (1 copy)
                                                                   Chief, WLRB (Biophysics Br.) (1 copy)
                                                                   Maj. D. A. Dowler (WLRP) (1 copy)
                                                                   Chief, WLRP (1 copy)
                                                                   WLDN (1 copy)
                                                                   WLR (1 copy)
                                                                   WLRTH, Capt. P. Fleming (1 copy)
                                                                   WLRB, Capt. J. E. Dieckhoner (1 copy)
                                                                   WLRB, Capt. D. Regenthaler (1 copy)
                                                                   WLIL (1 copy)
                                                                   Chief, WLRE (1 copy)
                                                                   WLRTH, Lt. J. S. Green (1 copy)
                                                                   WLRPX, Maj. H. F. Rizzo (1 copy)
                                                                   WLAA-3, Lt. J. Koziol (1 copy)

Air Force Western Test Range, AFSC, Vandenberg AFB, California 93437 Attn: Technical Library (1 copy)
                                                                           WTOSM (1 copy)

Aerospace Defense Command, Ent AFB, Colorado 80912 Attn: 90SD (Dir., Space Defense) (1 copy)
                                                          ADLDC, (DCS of Plans) (1 copy)
                                                          ADLMD-W (Missile & Space Weapons Pr.) (1 copy)
                                                          ADLPW, Maj. Douglas McComas (1 copy)
                                                          ADOOA, (Operations Analysis) (1 copy)
                                                          ADCSG, (Command Surgeon) (1 copy)

Division of McDonnell - Douglas Corp., 3000 Ocean Park Blvd., Santa Monica, California 90406 Attn: Department A2-260 Library (1 copy)
Dr. Barrett, Ch.-Nuc. Eff. Sect., A2-260 (1 copy)
M. Baier-Sp. Phys. & Planetary Sci. Br. (1 copy)
Ken. McClymonds (1 copy)
R. J. Reck (1 copy)
Dr. A. D. Goedeke, Space Sciences Dept. (1 copy)
Dr. O. K. Moe, Atmospheric Sciences Br. (1 copy)

William E. Drummond, Consultant, 3206 Greenlee Drive, Austin, Texas 78703 (1 copy)

Dynamic Science, 1900 Walker Avenue, Monrovia, Calif. 91016 Attn: Dr. J. C. Peck (1 copy)

Eastman Kodak Company, Kodak Park Works, Bldg. 65, Rochester, New York 14650 (1 copy)

EG&G Inc., 933 San Pedro, S. E., Albuquerque, New Mexico 87108 (1 copy)

EG&G Inc., 1501 Wilson Blvd., Arlington, Va. 22209 (1 copy)

EG&G Inc., P.O. Box 227, Bedford, Massachusetts 01730   Attn: Doc. Control Ctr. For Dr. M. Shuler (1 copy)

Dr. Neidhardt, 7449 N. Natchex Ave., Niles, Illinois 60648 (1 copy)

General Applied Science Labs., Inc., Merrick and Stewart Avenues, Westbury, Long Island, New York 11590 Attn: Master Document Control (1 copy)

General Dynamics/Convair, Lindbergh Field Plant, 3302 Pacific Highway, San Diego, Calif., 92101 (1 copy)

General Dynamics/Convair, 5001 Kearney Villa Road, P.O. Box 1128, San Diego, California 92112 Attn: Dr. D. A. Hamlin, MZ 595-00 (1 copy)
P. K. Rol, MZ 596-51 (1 copy)
R. H. Neynaber, MZ 596-61 (1 copy)
J. C. Nance (1 copy)
Library, 128-00 (1 copy)

General Dynamics Corporation, Electronics Division, 3090 Pacific Highway, San Diego, Calif. 92112 (1 copy)

General Dynamics/Electronics, 1400 North Goodman Street, Rochester, New York 14609 Attn: Technical Library (1 copy)

General Dynamics Corp., Fort Worth, P.O. Box 748, Fort Worth, Texas 76101 Attn: Technical Library

General Dynamics Corporation, Quincy Division, 97 E. Howard Street, Quincy, Mass. 02169 (1 copy)

General Dynamics Corporation, San Diego Office, 3302 Pacific Highway, San Diego, California (1 copy)

General Electric Company, 1 River Road, Schenectady, New York 12306 Attn: Dr. R. Kilb (1 copy)

General Electric Company, 100 Woodlawn Avenue, Pittsfield, Mass. 01201 (1 copy)

General Electric Company, Aerospace Electronics Dept., French Road, Utica, New York 13502 Attn: Technical Information Center (1 copy)

General Electric Company, Communication Products Department, Mountain View Road, Lynchburg, Virginia 24503 Attn: F. L. Hopkins, Appl. Eng. (1 copy)

General Electric Company, Defense Electronics Division, Court Street, Syracuse, New York 13201 Attn: Vic Gulick, Doc. Control, Rm. K3 (1 copy)
George H. Millman (1 copy)

Technical Services Co., Inc. 1331 H Street, NW, Washington, D.C. 20005 (1 copy)

General Electric Company, Tempo-Center for Advanced Studies, 816 State Street, Santa Barbara, California 93102 Attn: DASA Information and Analysis Center
(1 copy)
Dr. R. Christian, P. Fischer (2 copies)

General Electric Company, Wyatt Bldg., 777 14th Street, NW, Washington, D.C. (1 copy)

General Electric Company, X-Ray Department, 4855 W. Electric Avenue, Milwaukee, Wisc. 53201 (1 copy)

General Motors Corp., AC Electronics Division, 7929 South Howell Avenue, Oak Creek, Wisc., 53154 Attn: P. G. Chard (1 copy)

General Motors Corp., Allison Division, Los Angeles Zone Office, 888 North Sepulveda Blvd., El Segundo, Calif. 90245 (1 copy)

General Motors Corp., Defense Research Laboratories, AC Electronics Division, 6767 Hollister Avenue, Goleta, Calif., 93017 Attn: C. J. Maiden (1 copy)

Grumman Aircraft Engineering Corp., Bethpage, New York 11714 (1 copy)

Gulf General Atomic Inc., P.O. Box 1111, San Diego, California 92112 Attn: Chief, Tech. Information Services For-
Dr. V. A. J. Van Lint (1 copy)
Dr. J. Malmberg (1 copy)
Dr. Ben Turner (1 copy)
Library, Evan Miller (1 copy)
Dr. L. P. Pheard, John Jay Hopkins Lab. (1 copy)

Heliodyne Corporation, 1401 Wilson Blvd., Arlington, Va. 22209 (1 copy)

Heliodyne Corporation, 7810 Burnet Ave, Van Nuys, Calif. 91405 (1 copy)

Heliodyne Corporation, Div. of Kms Industries, Inc. 11689 Sorrento Valley Road, San Diego, Calif. 92121 (1 copy)

High Voltage Engineering Corp., Robert J. Van De Graaff Lab., Burlington, Massachusetts 01803 Attn: Dr. Andrew Wittkower (1 copy)

Holmes and Narver, Inc., 828 South Figueroa Street, Los Angeles, California 90017 Attn: Mr. F. Galbreath (1 copy)

Honeywell Incorporated, 1001 West Maude Avenue, Sunnyvale, Calif. 94086 (1 copy)

Litton Systems, Inc., Mellonics Systems Div., 335 Bearhill Road, Waltham, Mass. (1 copy)

Lockheed-Georgia Company, A Division of Lockheed Aircraft Corporation, 86 S. Cobb Drive, Marietta, Georgia 30061 Attn: Technical Library (1 copy)

Lockheed Missiles and Space Company, A Division of Lockheed Aircraft Corp., P.O. Box 504, Sunnyvale, California 94088
Attn: Dr. L. Fisher/Dept. 52-40/Bldg. 202 (1 copy)
RCS-RW/Dept. 55-54/Bldg. 570/E. N. Perry (1 copy)
N. Gamara, Dept. 58-41, Bldg. 130-1 (1 copy)
Dr. R. Varney/Dept. 52-40/Bldg. 201 (1 copy)
D. L. Kavanaugh (1 copy)
D. M. Nether/Dept. 81-23/Bldg. 154 (1 copy)
J. Klumpp (1 copy)
Art Hubbard (1 copy)
Dr. Rolf Landshoff (Dept. 52-10) (1 copy)
Dr. S. E. Singer (Palo Alto) (1 copy)
R. Meyerott (Palo Alto) (1 copy)
D. Holland (Palo Alto) (1 copy)
Dr. Martin Walt (Palo Alto) (1 copy)
Dr. L. D. Singletary (Palo Alto) (1 copy)
Dr. R. Meyerott (Palo Alto) (1 copy)
R. Munson (1 copy)

Lockheed Missiles and Space Company, 3251 Hanover Street, Palo Alto, Calif. 94304 Attn: Dr. S.E. Singer (1 copy)
Mr. R. Landis (1 copy)

Motorola, Inc., Government Electronics Div., 8201 E. Mc Donald Road, Phoenix, Arizona 85252 Attn: Mr. Roger Cox (1 copy)

Motorola, Inc., Semiconductor Products Div., 5005 East Mc Dowell Road, Phoenix, Arizona 85008 (1 copy)

Mount Auburn Research Associates, Inc., 12 Norfolk Street, Cambridge, Massachusetts 02139 Attn: Dr. E. Stubbs (1 copy)

The National Cash Register Co., South Main & K Street, Dayton, Ohio 45409 (1 copy)

National Co., Inc., 111 Washington Street, Melrose, Mass. 02176 (1 copy)

National Engineering Science Co., 709-11 Fair Oakes Ave., Pasadena, Calif. 91105 (1 copy)

National Fire Protection Association, 60 Battery March Street, Boston, Massachusetts 02110 Attn: Library (1 copy)

North American Rockwell Corp., Atomics International Division, 8900 DeSoto Street, Canoga Park, Calif. 91304 (1 copy)

Radio Corporation of America, Main Plant, Electronic Components and Devices, New Holland Ave., Lancaster, Penn. (1 copy)

Radioptics, Inc., Room 308, 238 Main Street, Cambridge, Mass. 02142 Attn: Dr. James G. Beckerley (1 copy)

The Rand Corporation, 1700 Main Street, Santa Monica, California 90406 Attn: Dr. R. LeLevier (1 copy)
Dr. Cullen Crain (1 copy)
Paul Tamarkin (1 copy)
Dr. W. Graham, Physics (1 copy)
Library (1 copy)
Dr. W. Graham (1 copy)
Dr. F. Gilmore (1 copy)
Dr. R.R. Rapp (1 copy)
Dr. E. Heffern (1 copy)
Dr. R. Latter (1 copy)
Dr. A.L. Latter (1 copy)
Dr. H. Borde (1 copy)
Dr. D.T. Griggs (1 copy)
Dr. W.J. Karzas (1 copy)
J.E. Whitener (1 copy)
Mr. W.B. Wright (1 copy)
Mr. F. Thomas (1 copy)

Rand Corporation, 1000 Connecticut Ave., N.W., Washington, D.C. 20036 (1 copy)

Raytheon Company, Boston Post Road, Wayland, Massachusetts 01778 Attn: Doc. Custodian for Richard Laurino (1 copy)

Surveys & Research Corporation, 1030 15th Street, N.W., Washington, D.C. 20005 (1 copy)

Sylvania Electric Products, Inc., 40 Sylvan Road, Waltham, Massachusetts 02154 Attn: Technical Library (1 copy)

Sylvania Electric Products, Inc., Electronic Systems Group, Western Div., 100 Ferguson Drive, P.O. Box 185, Mountain View, California 94040
Attn: Technical Documents Ctr./P. Slater (1 copy)

System Development Corporation, 2500 Colorado Avenue, Santa Monica, California 90406 Attn: Technical Library (1 copy)

System Development Corporation, 5720 Columbia Pike, Falls Church, Va, 20041 (1 copy)

System Sciences, Inc., 4720 Montgomery Lane, Bethesda, Maryland 20014 Attn: Mr. J.S. Smith (1 copy)

Systems, Science and Software, Inc., P.O. Box 1620, LaJolla, Calif. 92037 Attn: Robert S. Englemore (1 copy)
Dr. L. Schalit (1 copy)
Charles Dismukes (1 copy)
Dr. B. Freeman (1 copy)

DOCUMENT CONTROL DATA - R&D

(Security classification of title, body of abstract and indexing annotation must be entered when the overall report is classified)

1. ORIGINATING ACTIVITY *(Corporate author)*	2a. REPORT SECURITY CLASSIFICATION
Avco Everett Research Laboratory 2385 Revere Beach Parkway Everett, Massachusetts	Unclassified
	2b. GROUP

3. REPORT TITLE

RELEVANT LABORATORY EXPERIMENTS

4. DESCRIPTIVE NOTES *(Type of report and inclusive dates)*
Research Report 325

5. AUTHOR(S) *(Last name, first name, initial)*

Friedman, H. and Patrick R.

6. REPORT DATE November 1968	7a. TOTAL NO OF PAGES 35	7b. NO. OF REFS 3
8a. CONTRACT OR GRANT NO. DASA-01-67-C-0131 b. PROJECT NO.	9a. ORIGINATOR'S REPORT NUMBER(S) Research Report 325	
c. d.	9b. OTHER REPORT NO(S) *(Any other numbers that may be assigned this report)* DASA-2156	

10. AVAILABILITY/LIMITATION NOTICES

11. SUPPLEMENTARY NOTES	12. SPONSORING MILITARY ACTIVITY Defense Atomic Support Agency Washington, D.C.

13. ABSTRACT

An experiment has been designed to test the basic assumptions of a new model[3] which describes debris motion towards the northern conjugate region from high altitude nuclear explosions. The experimental facility consists of a coaxial plasma source which accelerates ionized aluminum into an environment where the background pressure and magnetic field can be controlled. The initial plasma velocity was 10 cm/μsec, the background magnetic field was varied from zero to 220 gauss and the pressure between 2μ and 50μ in air. These conditions are such that (1) ordinary momentum transfer collisions are unimportant (2) the magnetic pressure is negligible as compared to dynamic plasma pressure and (3) the only momentum exchange mechanism is charge exchange collisions in the presence of a magnetic field. Ultraviolet radiation from the plasma source preionizes the background gas producing an Alfven speed based on the ion density which is less than the plasma velocity. The ambient magnetic field is swept up by aluminum plasma and provides the mechanism for charge exchange momentum exchange process. We find that the aluminum plasma is decelerated with the addition of a magnetic field nearly parallel to the plasma motion. The deceleration rate is proportional to the background pressure. Finally, we note that the charge exchange pickup is effective even at relatively low magnetic fields where the air-ion gyro radius based upon initial plasma velocity is several times the plasma scale length.

DD FORM 1473
1 JAN 64

KEY WORDS	LINK A		LINK B		LINK C	
	ROLE	WT	ROLE	WT	ROLE	WT
1. Plasma physics						
2. Shock waves						
3. Laboratory simulation of high altitude plasma motion						

INSTRUCTIONS

1. ORIGINATING ACTIVITY: Enter the name and address of the contractor, subcontractor, grantee, Department of Defense activity or other organization (corporate author) issuing the report.

2a. REPORT SECURITY CLASSIFICATION: Enter the overall security classification of the report. Indicate whether "Restricted Data" is included. Marking is to be in accordance with appropriate security regulations.

2b. GROUP: Automatic downgrading is specified in DoD Directive 5200.10 and Armed Forces Industrial Manual. Enter the group number. Also, when applicable, show that optional markings have been used for Group 3 and Group 4 as authorized.

3. REPORT TITLE: Enter the complete report title in all capital letters. Titles in all cases should be unclassified. If a meaningful title cannot be selected without classification, show title classification in all capitals in parenthesis immediately following the title.

4. DESCRIPTIVE NOTES: If appropriate, enter the type of report, e.g., interim, progress, summary, annual, or final. Give the inclusive dates when a specific reporting period is covered.

5. AUTHOR(S): Enter the name(s) of author(s) as shown on or in the report. Enter last name, first name, middle initial. If military, show rank and branch of service. The name of the principal author is an absolute minimum requirement.

6. REPORT DATE: Enter the date of the report as day, month, year; or month, year. If more than one date appears on the report, use date of publication.

7a. TOTAL NUMBER OF PAGES: The total page count should follow normal pagination procedures, i.e., enter the number of pages containing information.

7b. NUMBER OF REFERENCES: Enter the total number of references cited in the report.

8a. CONTRACT OR GRANT NUMBER: If appropriate, enter the applicable number of the contract or grant under which the report was written.

8b, 8c, & 8d. PROJECT NUMBER: Enter the appropriate military department identification, such as project number, subproject number, system numbers, task number, etc.

9a. ORIGINATOR'S REPORT NUMBER(S): Enter the official report number by which the document will be identified and controlled by the originating activity. This number must be unique to this report.

9b. OTHER REPORT NUMBER(S): If the report has been assigned any other report numbers (either by the originator or by the sponsor), also enter this number(s).

10. AVAILABILITY/LIMITATION NOTICES: Enter any limitations on further dissemination of the report, other than those imposed by security classification, using standard statements such as:

(1) "Qualified requesters may obtain copies of this report from DDC."

(2) "Foreign announcement and dissemination of this report by DDC is not authorized."

(3) "U. S. Government agencies may obtain copies of this report directly from DDC. Other qualified DDC users shall request through
_____ ."

(4) "U. S. military agencies may obtain copies of this report directly from DDC. Other qualified users shall request through
_____ ."

(5) "All distribution of this report is controlled. Qualified DDC users shall request through
_____ ."

If the report has been furnished to the Office of Technical Services, Department of Commerce, for sale to the public, indicate this fact and enter the price, if known.

11. SUPPLEMENTARY NOTES: Use for additional explanatory notes.

12. SPONSORING MILITARY ACTIVITY: Enter the name of the departmental project office or laboratory sponsoring (paying for) the research and development. Include address.

13. ABSTRACT. Enter an abstract giving a brief and factual summary of the document indicative of the report, even though it may also appear elsewhere in the body of the technical report. If additional space is required, a continuation sheet shall be attached.

It is highly desirable that the abstract of classified reports be unclassified. Each paragraph of the abstract shall end with an indication of the military security classification of the information in the paragraph, represented as (TS), (S), (C), or (U).

There is no limitation on the length of the abstract. However, the suggested length is from 150 to 225 words.

14. KEY WORDS: Key words are technically meaningful terms or short phrases that characterize a report and may be used as index entries for cataloging the report. Key words must be selected so that no security classification is required. Identifiers, such as equipment model designation, trade name, military project code name, geographic location, may be used as key words but will be followed by an indication of technical context. The assignment of links, rules, and weights is optional.

Defense Threat Reduction Agency
45045 Aviation Drive
Dulles, VA 20166-7517

CPWC/TRC   November 3, 1999

MEMORANDUM FOR DEFENSE TECHNICAL INFORMATION CENTER
             ATTN: OCQ/MR WILLIAM BUSH

SUBJECT: DOCUMENT CHANGES

     The Defense Threat Reduction Agency Security Office
has performed a classification/distribution statement
review for the following documents:

     DASA-2519-1, AD-873313, STATEMENT A
     DASA-2536, AD-876697, STATEMENT A
     DASA-2519-2, AD-874891, STATEMENT A
     DASA-2156, AD-844800, STATEMENT A
     DASA-2083, AD-834874, STATEMENT A
    -DASA-1801, AD-487455, STATEMENT A
     POR-4067, AD-488079, STATEMENT C,
ADMINISTRATIVE/OPERATIONAL USE
     DASA-2228-1, AD-851256, STATEMENT C, *No Target*
ADMINISTRATIVE/OPERATIONAL USE   *only chged from S A to adm/oper.*
     RAND-RM-2076, AD-150693, STATEMENT D,
ADMINISTRATIVE/OPERATIONAL USE
   7* AD-089546, STATEMENT A, ADMINISTRATIVE/OPERATIONAL USE * *ST-A*
    -DASA-1847, AD-379061, UNCLASSIFIED, STATEMENT C,   *Jun'65*
ADMINISTRATIVE/OPERATIONAL USE
     RAND-RM-4812-PR, ELEMENTS OF A FUTURE BALLISTIC *370168*
MISSILE TEST PROGRAM, UNCLASSIFIED, STATEMENT C,   *(Cert)*
ADMINISTRATIVE/OPERATIONAL USE

     If you have any questions, please call me at 703-325-
1034.

Leave ST-A
per a. Jarrett
23 nov 99

                              Ardith Jarrett
                              ARDITH JARRETT
                              Chief, Technical Resource Center